Sustain. Water Resour. Manag. (2015) 1:189–211
DOI 10.1007/s40899-015-0019-2

ORIGINAL ARTICLE

Water quality of the Helvetian and Eocene aquifers in Al Zerba catchment and southern parts of Al Qweek Valley, Aleppo basin, Syria

Rudy Abo[1] · Broder J. Merkel[1]

Received: 24 May 2015 / Accepted: 21 August 2015 / Published online: 30 August 2015

Abstract Groundwater is a key factor for sustainable socio-economic development in arid and semi-arid countries. The study area constitutes the south and southwestern parts of Aleppo basin, north of Syria. It is characterized by semi-arid climate and limited water resources. The aims of this study are to evaluate the groundwater quality with concern to drinking and irrigation suitability, water–rock interaction, and potential source rock to assess the main hydrochemical processes controlling chemical composition of groundwater in the Neogene and Paleogene aquifer systems. Hydrochemical data of 29 irrigation and observation wells distributed in the region were used in this study. Concentrations of the dominant ions are following the order $Na^+ > Ca^{2+} > Mg^{2+} > K^+$ and $HCO_3^- > Cl^- > SO_4^{2-}$ for major cations and anions, respectively. Ca–Na–HCO_3, Na–Ca–SO_4, and Ca–Na–Cl are the main groundwater types in the region. The graphical interpretation and cluster analysis of groundwater samples identified three main hydrochemical facies in the region. These groups are differentiated by three levels of total dissolved solids (TDS) value ranges from 390 mg/l for the group A, 742 and 1795 mg/l for the group B and C, respectively. The results also show that most of the groundwater samples are close to saturation or oversaturation with respect to the minerals: aragonite, calcite, and dolomite, while halite and gypsum are always under-saturated. Furthermore, the inverse geochemical modeling of groundwater samples indicates three main processes that are responsible for groundwater evolution in the region: plagioclase weathering (albite, hypersthene), de-dolomitization, and cation exchange. These processes increase in groundwater salinity from the east to the southwestern parts of the study area. The groundwater in the region is partly critical for drinking and irrigation due to the high average TDS (925 mg/l), nitrate (43.78 mg/l), and salinity. However, groundwater samples exhibited low sodium adsorption ratios, moderate magnesium hazard, and low residual sodium carbonate. Despite of that, this type of water can adversely affect the soil and crops yields in the long term and prevent a sustainable development of agriculture in the region of interest.

Keywords Aleppo Basin · Water quality · Saturation index · Dissolution · Salinity hazard · Inverse modeling · PHREEQC

Introduction

Groundwater is one of the most important sources for drinking water and irrigation in arid and semi-arid environments, where limited renewable water resources, low average annual precipitation, and high evaporation rates are dominant. Based on this fact, the management of groundwater resources requires adequate knowledge of the distribution of groundwater-bearing horizons and their interaction with different components of the hydrogeological system. Furthermore, groundwater development involves other important factors such as groundwater abstraction, groundwater recharge, and water quality. Nowadays, the quality of groundwater is one of the most important characteristics for sustainable planning of agricultural, economic, and other human activities particularly in arid and semi-arid countries. In such environments,

✉ Rudy Abo
rudy.abo@hotmail.de

[1] Department of Hydrogeology, TU Bergakademie Freiberg, Freiberg, Germany

over-exploitation of groundwater resources often led to significant decline in groundwater tables, transient flow, saline water intrusion, mixing water from different hosting formations, soil salinity, and many adverse effects on groundwater quality (Custodio 2002; Luijendijk 2003; Luijendijk and Bruggeman 2008; Al-Charideh 2012).

Consequently, the quality of water used for agriculture has direct impact on the soil fertility and crop yield (Li et al. 2013) and thus the exhaustion of groundwater resources and soil salinization is one of most important challenges facing the governments in these regions (Hagi-Bishow 1998; Edmunds and Droubi 1998; Edmunds 2003). For instance, a sustainable increase in salinity/sodicity of irrigation water can reduce the infiltration downwards through the soil profile and hence the available water in the intake zone to the crops. Moreover, the accumulation of ions such as Na^+, Cl^-, and B in both water and soil in elevated concentrations can led to crop hazards (Ayers and Westcot 1985). Generally, groundwater poses a strategic stock for drinking water in many countries of the Middle East. Nevertheless, it can easily be contaminated by various anthropogenic activities, aquatic microbiological organisms, or gradual changes in composition along its movement path (water–rock interactions), and thus, becomes an unsuitable source for drinking water or even for irrigation. Water quality criteria, including scientific information and toxicity data, were derived in the few years by a number of large organizations such as the US environmental protection agency (EPA) and the world health organization (WHO) to protect human health and aquatic life (Hiscock and Bense 2014). In 1994 and 2003, the Syrian Arab Organization for Standardization and Metrology (SASMO) adopted the Syrian national standard for drinking and irrigation water and published them under the standards No. 45 and 2752, respectively (http://www.sasmo.org.sy/en/search_standards). The standards specified general conditions required for water to be potable for use in drinking and agricultural activities, including physical and chemical criteria and the maximum contaminant level (MCL) of organic/inorganic, metals, trace elements, and microbiological contaminants in water. In addition, a summary of adopted drinking water quality standards in the Eastern Mediterranean region was provided by the WHO (2006).

Although groundwater consumption in agriculture and industrial activities is embedded in the water regulation in many developing countries (Kalf and Woolley 2005), water quality issues remain the common concern, particularly in arid and semi-arid regions. For instance, the accelerated socio-economic development in the semi-arid regions of Syria, and the increasing demand on water for irrigation led to the over-exploitation of groundwater and continuous decline of an important part of the strategic reserve of the country (Luijendijk and Bruggeman 2008). Over the last three decades, agriculture was a most important sector of the economy in the country and had the first priority of all development projects as a major supply of the gross national product (GNP). As a traditional agricultural country, about 90 % of all water resources in Syria are used for irrigation, while only 10 % is used for industrial production and domestic domain (BGR and MOI 2004; Berndtsson and Mourad 2012; Abo and Merkel 2015). The expansion of irrigated areas in the last few years raises the need for better management for water resources in the basins and effective sustainable development of water quality in the future. However, the hydrogeological systems of Aleppo basin have been intensively investigated in the last decade due to its economic and agriculture importance. A large number of these studies focused on the isotopic and groundwater management issues of the upper cretaceous aquifer conducted by Wolfart (1966), GCHS (1999), ICARDA (2000), Stadler et al. (2012), and Al-Charideh (2012), while only a view studies addressed the groundwater quality problems of the upper aquifers such as those accomplished by Selkhozpromexport (1979), (JICA 1997), Luijendijk (2003) and Luijendijk and Bruggeman (2008).

The objectives of this study were to assess the groundwater quality, source rock deduction, and the main hydrochemical mechanisms affecting the groundwater constituents of the Neogene and Paleogene aquifers in Al Qweek valley and Al Zerba catchment area. The study also aimed to investigate the suitability of groundwater for drinking and agricultural activities in the region.

Study area

Location and climate

The study area covers 1987 km^2 of the central and south-western parts of Aleppo basin. It is situated at an average elevation of 330 m m.a.s.l (from 260 to 430 m) and extends from the longitude of 36°80′E–37°23′E and latitude of 35°82′N–36°27′N (Fig. 1). The region is dominated by flat topography with an average slope range from 7 to 8 %. The area is also characterized by a prevailing Mediterranean semi-arid climate with four distinct seasons. The average annual precipitation ranges from 240 mm in the east (Aleppo City and Al Hass Mountain) to 350 mm in the western parts of the study area (Tel Hadya) and relatively high average potential evapotranspiration that can reach up to 1800 mm/year (Luijendijk and Bruggeman 2008; Abo and Merkel 2015). Typical is a cold winter and a long hot summer with monthly average temperature ranging from 8 to 27 °C, respectively, and a mean annual temperature of 18.1 °C.

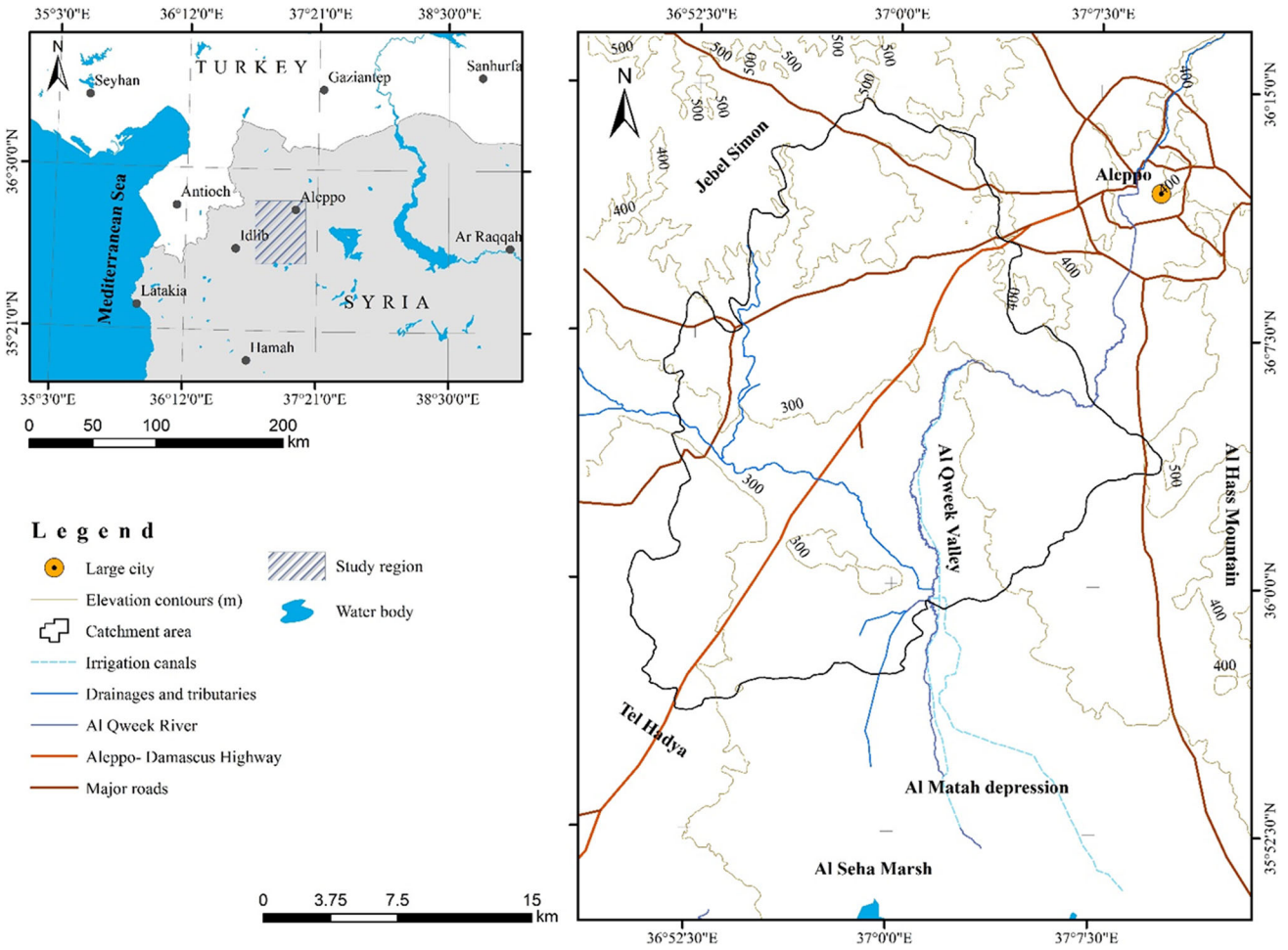

Fig. 1 The location of the study area

Geology and hydrogeological setting

The geology of Syria and Aleppo basin has been described by Ponikarov (1964) and the geological and hydrogeological survey of Selkhozpromexport (1979). A simplified geological map of the study area is shown in Fig. 2. Three main stratigraphic units can be distinguished in almost all sections of Aleppo basin: the Helvetian (N_1h), the Eocene (Pg_2^{2+3}), and the Pleistocene sediments (Q_3 and Q_4). The Neogene/Helvetian deposits constitute the most prevalent outcrops in the region. They are mainly determined by organogenous limestone interbedded with an important thickness of Helvetian basalt in the east with an average thickness ranging from 10 to 50 m in Al Hass area. The Helvetian formations overlie unconformable with the Paleogene/Middle and Upper Eocene deposits. Lithologically, the Eocene formations are characterized by soft, loose limestones interbedded with hard clayey limestone. They cover a considerable area in the south and southeastern parts of the region with a total thickness varying between 50 and 120 m (Selkhozpromexport 1979). The Upper Pleistocene sediments (Q_3 and Q_4) cover the central parts of the study area. They consist of lacustrine, proluvial, and alluvial deposits. They are mainly determined by pebbles, loam, sand, and gypsum, filling the entire area of Al Qweek Valley and Al Matah Depression along the neighboring foothills with an average thickness of 15 m (Luijendijk 2003). The hydrogeology of Aleppo basin was described by Wolfart (1966), Selkhozpromexport (1979), Gruzgiprovodkhoz (1982), and Brew et al. (2001). The hydrogeological units consist of three main aquifers. *The deep confined aquifer* of the Upper Cretaceous formation (Cenomanian–Turanian) is determined by dolomitized limestone with an approximate thickness of 250-350 m; the overlaying layer consists of marl, clay, and chalky limestone of the Maastrichtian–Danian and Paleocene sediments as an aquitard with a total average thickness of 420–520 m (Stadler et al. 2012). The Upper Cretaceous aquifer is characterized by high groundwater productivity and brackish water with elevated concentrations of Ca^{2+},

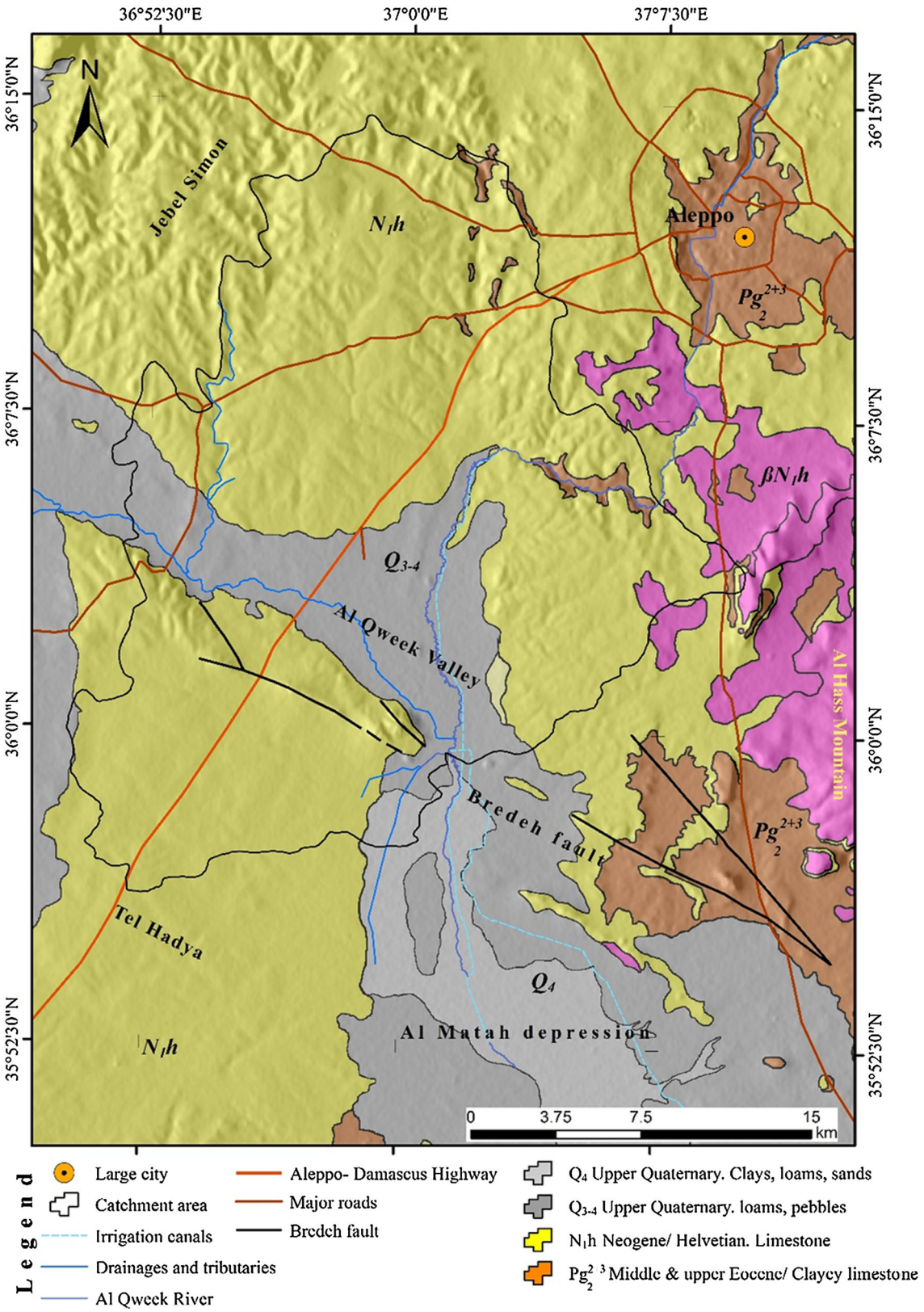

Fig. 2 The 1:200,000 geological maps of study area simplified after Ponikarov (1964)

SO_4^{2-}, and Na^+, indicating gypsum and halite dissolution processes (Al-Charideh 2012). *The middle unconfined aquifer* is determined by alternation of limestone and clayey limestone of the Middle and Upper Eocene. The average thickness ranges from 40 m in the east to 100 m in the Al Qweek valley, according to UN-ESCWA (1997). The groundwater in this aquifer varies considerably from fresh to brackish water. The hydrochemical investigation of Al-Charideh (2012) and Stadler et al. (2012) suggests a hydraulic connection between the Cretaceous water bearing horizons and the Paleogene aquifer. The *uppermost unconfined aquifer* is identified by the Neogene aquifer system and determined by hard fractured limestone of the Helvetian formation. According to the survey of Selkhozpromexport (1979), the aquifer has high productivity, high permeability, and low mineralized water. Unfortunately, this aquifer is almost exhausted by heavy exploitation during the last few decades and, thus, significant changes in water quality are expected. As reported by Wolfart (1966), Gruzgiprovodkhoz (1982), JICA (1997), Luijendijk and Bruggeman (2008), and Abo and Merkel (2015), the average annual groundwater recharge in the region ranges from 10 to 60 mm/year which is about 10 % of the annual precipitation. The outcropping formations, Helvetian limestone in the north and the basalt flow in the eastern parts of the study area are rather permeable and thus suggested by many previous studies as recharge areas (Luijendijk and Bruggeman 2008; Stadler et al. 2012).

Materials and methods

Data from 29 groundwater samples were used in this study for the assessment of groundwater quality, interpretation of the hydrochemical data, and the dominant geochemical processes. The data include major chemical groundwater constituents of the upper and middle aquifers. Published and unpublished reports were used in this study providing general representation about the hydrochemical conditions in the region of interest (Table 1). Chemical and physical parameters of water samples collected from irrigation and observation wells were assessed during fieldwork conducted by the ICARDA team in 2001–2005, and throughout the water development project of Aleppo basin in 2002–2011 (Phase 1 and 2) directed by the Syrian Ministry of Irrigation (MOI) in cooperation with the Federal Institute for Geosciences and Natural Resources (BGR). The total depth of irrigation wells ranges from 90 to 295 m with an average depth of 165 m. The chemical laboratory analysis of major ions of ICARDA samples was conducted using the standard procedures reported by Ryan et al. (2001). According to Luijendijk and Bruggeman (2008), flame photometry was used to determine Na^+ and K^+, while Ca^{2+}, Mg^{2+}, NO_3^-, and Cl^- were determined by titration and barium sulfate precipitation for SO_4^{2-}. The general hydrochemical constituents of the Eocene collected groundwater samples (J–well ID) were analyzed using an ion chromatograph (IC) at the laboratories of the Syrian Atomic Energy Commission (SAEC) (Al-Charideh 2012). The groundwater samples from the HC–Boreholes were analyzed in the laboratory of the General Company of Hydraulic Studies (GCHS) in cooperation with the Federal Institute for the Geosciences and Natural Resources (BGR), using the standard analysis procedures documented by Droubi (1983), (Stadler et al. 2012). Analytical quality was checked by anion–cation balance and comparing total dissolved solids (TDS) with the electrical conductivity (EC). The analysis of groundwater samples was assumed to be acceptable when the calculated balance was in the range 5–10 % and the TDS/EC ratio was between 0.55 and 0.76 (Hounslow 1995; Appelo and Postma 2005). Figure 3 shows the local distribution of the groundwater samples in the study area.

Saturation indices and hydrochemical facies

Saturation indices (SI) and ion activities were calculated using PHREEQC program v.2 (Parkhurst and Appelo 1999) and Waterq4f database (Ball et al. 1987). An SI value equal or close to zero indicates saturation with a

Table 1 The source of data

Author/association	Type of data	Samples ID	Sampling period
Adriana Bruggeman (ICARDA)	Spreadsheet of complete general hydrochemical analysis	N1–17	2001–2004
Luijendijk Elco	Spreadsheet of general analysis, thesis	N1–17	2003
Al-Charideh	Published data	P3–8	2012
BGR (Federal Institute for Geosciences and Natural Resources)	Spreadsheet, spatial data and general analysis with report	P1–2 P9–12	2011
BGR and MOI (Syrian Ministry of Irrigation)	Spreadsheet, well spatial data and groundwater level	Observation and irrigation wells	2002–2004

specific mineral, while a negative value means that the water is unsaturated with respect to a certain mineral phase. Thus, dissolution of this mineral can be expected. If $SI > 0$, then the water is assumed to be oversaturated with the mineral phase, and thus, precipitation of the mineral is possible. Furthermore, the hydrochemical facies and potential mixing between the Helvetian and Eocene aquifers are also discussed by means of the Piper trilinear diagram (Piper 1944) and cluster analysis. In hydrogeology, cluster analysis is one of common techniques uses to classify groundwater observations into statistically distinct groups based on their similar hydrochemical characteristics. In this study, hierarchical cluster analysis was performed to determine whether groundwater samples are statistically classified into distinct hydrochemical groups. WARD's algorithm was used as a linkage method between similar observations with Euclidean distance. This procedure was followed by significance test checking the correlation between the defined variables within each classified group. On the other hand, the development of dissolution/precipitation processes, de-dolomitization, and ion exchanges between existing minerals in groundwater samples with hosted rocks were also investigated by graphical interpretation of the relationship between major anions and cations of Na^+/Cl^-, $Ca^{2+}/SO_4{}^{2-}$, and Mg^{2+}/Ca^{2+} on scatter plots. For instance, sodium chloride (halite) is considered as the major source for Na^+ and Cl^-. If the concentration of Cl^- anions is greater than Na^+, then a reverse ion exchange is expected. In contrast, when Na^+ concentration is higher than Cl^-, then another source for Na^+ such as albite can be expected. Equal amounts of chlorine and sodium in groundwater indicate a dissolution process of the halite hosting rocks Hounslow (1995). Similarly, when Ca^{2+} concentration in groundwater is less than $SO_4{}^{2-}$, then pyrite oxidation or Ca^{2+} removal by calcite precipitation may be the reason for this, while higher concentrations indicate another source for Ca^{2+} than gypsum, such as calcite and dolomite. Moreover, Mg^{2+}/Ca^{2+} relationship is very important in carbonate aquifers. It provides initial indicators about the dissolution of dolomite at high Mg^{2+}/Ca^{2+} ratios, while Ca^{2+} is removed gradually from the groundwater when the ratio is equal to one.

Groundwater evolution

Dissolved constituents in the groundwater provide fingerprints on its geologic history (Freeze and Cherry 1979). The available techniques to identify the origin of different types of groundwater using their initial chemical composition can be very helpful understanding the water–rock reactions, particularly when the source rock is unknown (Hounslow 1995). Gibbs (1970) suggested a graphical method to explain groundwater evolution mechanisms and the functional sources of dissolved chemical constituents as a relationship between the TDS and both $Na^+/(Na^+ + Ca^{2+})$ and $Cl^-/(Cl^- + HCO_3{}^-)$ ratios. In this study, the source rocks of the upper and middle aquifers were deduced using six different indices which are explained comprehensively by Hounslow (1995). These indexes are as follows:

Plagioclase weathering index:
$$\frac{(Na^+ + K^+ - Cl^-)}{(Na^+ + K^+ + Cl^- + Ca^{2+})}.$$

Sodium/Chloride index:
$$\frac{Na^+}{(Na^+ + Cl^-)} \text{ TDS dependence.}$$

Carbonate weathering/dissolution:
$$\frac{Ca^{2+}}{(Ca^{2+} + SO_4^{2-})} \text{ pH dependence.}$$

Silicate/Carbonate weathering: TDS.

Rock weathering/evaporation:
$$\frac{Cl^-}{\sum \text{anions}} \text{TDS must be considered.}$$

Gypsum dissolution, brine/carbonate or silicate weathering:
$$\frac{HCO_3^-}{\sum \text{anions}}.$$

Inverse modeling (PHREEQC)

In addition to the graphical methods, groundwater evolution and different rock–water interaction processes were investigated using geochemical inverse modeling with PHREEQC which attempts to determine the phases mole transfers between one or different mixture ratio of initial solutions and final water based on a mass balance approach (Plummer and Back 1980). Therefore, adequate information about chemical composition of the end-member water and the first-order process of mixing are required to reduce uncertainty in the calculation of mole mass transfers (Appelo and Postma 2005; Carucci et al. 2012). In this study, the geochemical inverse modeling was performed to investigate the de-dolomitization and ion exchange processes throughout the upper aquifer in addition to the study of groundwater development by weathering processes in the recharge area.

Inverse modeling was optimized to have a minimal number of models reducing the large number of results by minimizing uncertainties for the input parameters. Furthermore, the modeled phases were limited to the dominant minerals in the study area. The first model reproduces the geochemical evolution and the potential plagioclase

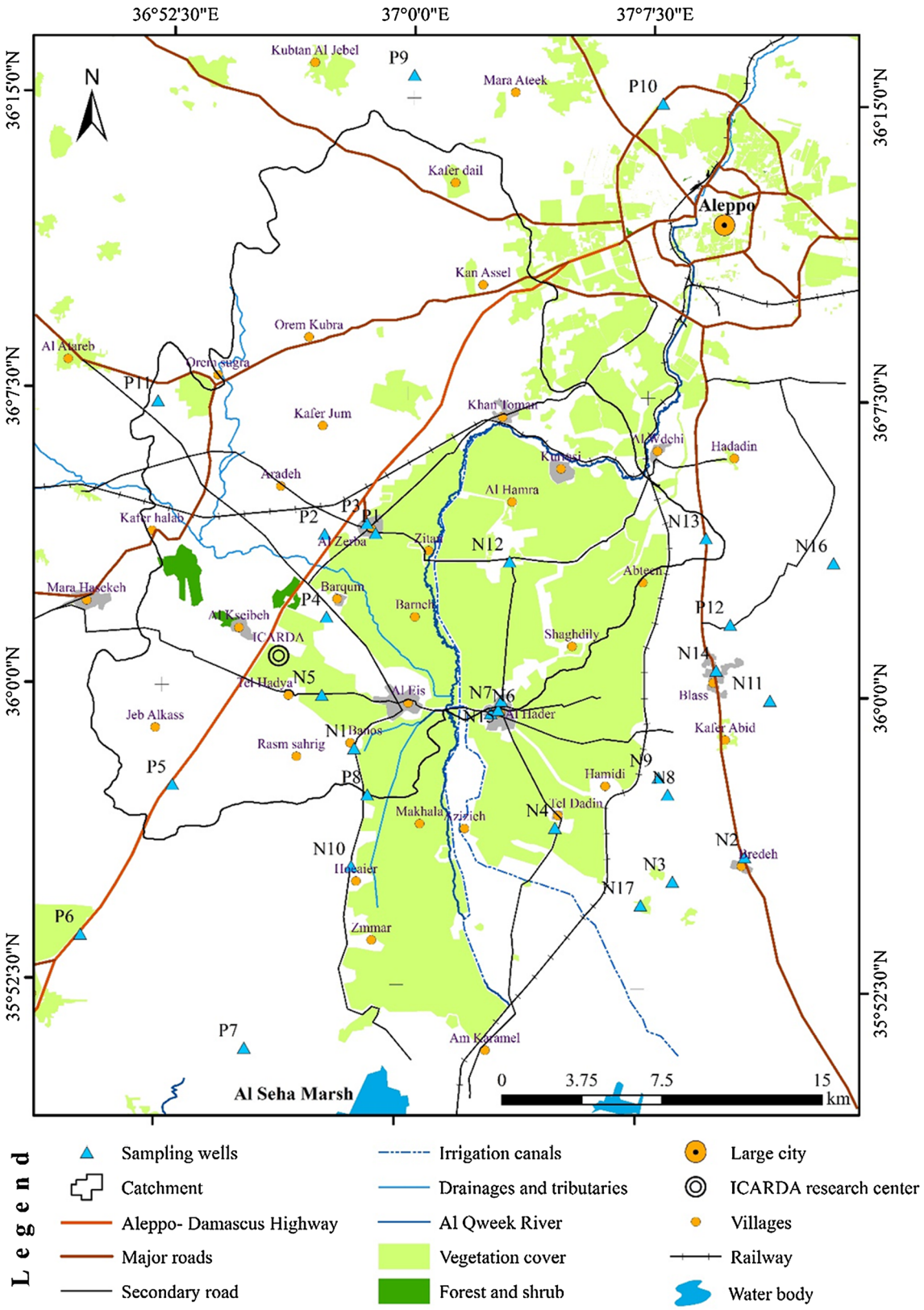

Fig. 3 The location of groundwater sampling points

weathering in the recharge area. According to the previous conducted studies in the region, weathering of sodium-rich plagioclase (albite) in the Miocene basalt is expected as a secondary source of sodium ions in groundwater (Selkhozpromexport 1979; Luijendijk 2003; Al-Charideh 2012). Generally, weathering of silicate minerals is a rather slow process resulting in gradual changes of the groundwater composition. These changes are less prominent in comparison to those in carbonate aquifers. Nevertheless, weathering of plagioclase minerals can release additional amount of sodium into groundwater by dissolution processes of albite. This leads to the preferentially formation of clay minerals such as montmorillonite covering the basalt rocks in particular in arid and semi-arid regions with low precipitation (slow flushing rate) and large groundwater residence time (Appelo and Postma 2005). Hence, the first model assumes typical interaction between rainwater (first solution) and groundwater of the upper aquifer (final solution). As mentioned above, the groundwater recharge constitutes about 10 % of the annual precipitation, while the residual precipitation (~90 %) is being removed by evaporation, root water uptake and surface runoff. Since evaporation and precipitation occur at the ground surface, the partial pressure of carbon dioxide and oxygen was adjuster to be equal to atmosphere pressure of $10^{-3.5}$ and $10^{-0.7}$ bar, respectively. The chemical analysis of precipitation samples was used for inverse modeling as initial water. These samples were collected from the southern parts of the study area for the winter season 2004 (Tel Hadya). The chemical analyses were conducted by the Syrian Ministry of Irrigation (MOI). Table 2 presents the general chemical analysis of precipitation sample. Because the mineral composition of the rocks is a key factor affecting water chemistry, three detailed bulk chemical analyses of the basalt samples in the recharge area were used to identify their mineral constitution using the NORM4 interpretation program (http://minerva.union.edu/hollochk/c_petrology/norms.htm). Table 3 lists the major chemical composition of the Miocene basalt in the region (Ma et al. 2013). The geochemical inverse model suggests the dissolution of plagioclase and hypersthene, the precipitation of Ca-montmorillonite, hematite, and diopside as the dominant minerals phases. The second and third models reproduce the geochemical path along the intermediate zone between the hydrochemical facies A and B, and the geochemical process along the flowpath between the groups B and C (end-member water). Calcite, dolomite, gypsum, organic matter (CH_2O), $CO_{2(g)}$ mineral, and gas phases, as well as the Ca/Na_2 and NaX cation exchange were considered in the modeling. The uncertainty used in the models is 0.1 for the pH value and 0.02–0.05 for the rest of the major elements in the solution. Due to the lack of data about the end-member groundwater, modeling of the potential mixing between the Neogene and Paleogene aquifers was not performed in this study.

Table 2 General chemical analysis of precipitation sample in the southern part of Aleppo, winter season 2004

	pH	*T* (°C)	Ca^{2+}	Mg^{2+}	Na^{+}	K^{+}	SO_4^{2-}	Cl^{-}	HCO_3^{-}	NO_3^{-}
Concentration (ppm)	6.4	12.9	10.4	1.2	5.9	0.01	29.6	7.09	12.2	1.33

Table 3 Bulk-rock major element compositions (wt%) of the Miocene basalt flow in the study area according to Ma et al. (2013)

Sample	JEH-01		JEH-03		JEH-05	
Location	Lat. 36°07′36″	Long. 37°09′18″	Lat. 36°06′11″	Long. 37°12′25″	Lat. 35°59′53″	Long. 37°10′40″
SiO_2	49.9		51.3		52.6	
TiO_2	1.6		1.7		1.5	
Al_2O_3	134		13.9		13.68	
Fe_2O_3	11.5		11.7		11.3	
MnO	0.08		0.09		0.08	
MgO	10.7		7.8		8.2	
CaO	7.2		7.9		7.7	
Na_2O	2.5		3.1		2.9	
K_2O	0.8		0.5		0.5	
P_2O_5	0.2		0.2		0.1	
LOI (loss on ignition)	1.7		0.5		0.65	

Groundwater suitability

For drinking water quality tests, the chemical composition of groundwater samples was compared to the water quality guidelines and standards of both USEPA (2002) and WHO (2011). Moreover, groundwater suitability for irrigation activities was investigated using the common available methods for water quality assessment such as sodium adsorption ratio (SAR), exchangeable sodium ratio (ESR), magnesium hazard (MH), residual sodium carbonate (RSC), and corrosion ratio (CR).

Sodium adsorption ratio (SAR)

The SAR of water proposed by Richards (1954) is

$$\mathrm{SAR} = \frac{\mathrm{Na}^{+}}{\sqrt{\frac{\mathrm{Ca}^{2+}+\mathrm{Mg}^{2+}}{2}}}, \tag{2}$$

where all ion concentrations are expressed in meq/l.

SAR is an indicator for both water and soil sodicity and measures the degree of the replacement of Na^{+} with $Ca^{2+} + Mg^{2+}$ in the soil. A high SAR value in water can damage the soil structure and later reduce crops productivity.

Exchangeable sodium ratio (ESR)

The term of exchangeable sodium percentage (ESP) can be determined by the amount of adsorbed sodium on the soil exchange matrix or in a solution (groundwater) as a proportion of cations exchange capacity in milliequivalents per 100 g of soil (Ayers and Westcot 1985). The exchangeable sodium ratio is a very important index to characterize the hazard of irrigation water on soil and crops. It is commonly given by the following formula (Lloyd and Heathcote 1985):

$$\mathrm{ESR} = \frac{\mathrm{Na}^{+}}{\mathrm{Ca}^{2+} + \mathrm{Mg}^{2+}}, \tag{3}$$

where all ionic concentrations are expressed in meq/l.

Several studies showed a linear relationship between ESR and the SAR index (Harron et al. 1983). The earlier research was conducted by the U.S. Salinity Laboratory staff (USSL). They proposed a linear equation to express the relationship between the measured exchangeable sodium ratio and the measured SAR in a solution phase (Richards 1954):

$$\mathrm{ESR} = -0.0126 + 0.01475 \times \mathrm{SAR} \quad \left(r^2 = 0.852\right). \tag{4}$$

However, water with an ESR value of above 0.30 is assumed to have an adverse impact on the growth of sensitive crops (high sodicity hazard).

Magnesium hazard (MH)

The MH was proposed by (Szabolcs and Darab 1964), and can be calculated according to the following equation (Paliwal 1972):

$$\mathrm{MH} = \frac{\mathrm{Mg}^{2+}}{\mathrm{Ca}^{2+} + \mathrm{Mg}^{2+}} \times 100, \tag{5}$$

where all ion concentrations are expressed in meq/l.

Generally, high concentration of Mg^{2+} in groundwater has adverse effects on agriculture and can lead to low crop yields and increase soil salinity (Joshi et al. 2009; Asiwaju-Bello et al. 2013). Water samples with MH values less than 50 % can be used for irrigation (Ayers and Westcot 1985).

Residual sodium carbonate (RSC)

Another indicator of sodium hazard is known as the RSC or bicarbonate hazard index. The empirical parameter was devised by Eaton (1950), assuming that calcium and magnesium would precipitate from water:

$$\mathrm{RSC} = \left[\mathrm{CO}_3^{2-} + \mathrm{HCO}_3^{-}\right] - \left[\mathrm{Ca}^{2+} + \mathrm{Mg}^{2+}\right], \tag{6}$$

where all ionic concentrations are expressed in meq/l.

Water with a high concentration of HCO_3^{-} and positive RSC loses its calcium and magnesium cations gradually from soil solution by precipitation, increasing at the same time the soil sodicity with sodium bicarbonates (Sadashivaiah et al. 2008). In contrast, a negative RSC value indicates that the accumulation of sodium is unlikely since sufficient amount of calcium and magnesium is in excess of what can be precipitated as carbonate. Therefore, groundwater with an RSC value above 2.50 meq/l is not suitable for irrigation activities and indicates hazards in soil structure (Hopkins et al. 2007; Nishanthiny et al. 2010). Generally, arid and semi-arid regions have high RSC values (Prasad et al. 2001).

Results and discussion

General hydrochemical characteristics

Physical parameter, major ions of groundwater samples, and water types are compiled in Table 4. The temperature of the collected groundwater samples of the Helvetian aquifer varies from 13.6 to 25.1 °C, and an average temperature of 22.2 °C. In contrast, the Eocene water samples exhibit relatively lower temperature changes than the upper aquifer ranges from 19 to 29 °C. The mean measured temperature for the Eocene groundwater is 23.3 °C. On the other hand, the pH value of the water samples ranges from 7.1 to 8.4, indicating a dominant

Table 4 General chemical composition and field physical parameters of groundwater samples of the Helvetian and Eocene aquifers

Well ID	Sample ID (Map no.)	Aquifer	pH	*T* (°C)	TDS (mg/l)	Ca^{2+} (mg/l)	Mg^{2+} (mg/l)	Na^{+} (mg/l)	K^{+} (mg/l)	HCO_3^{-} (mg/l)	SO_4^{2-} (mg/l)	Cl^{-} (mg/l)	NO_3^{-} (mg/l)	Water type
23	N1	Helvetian	8.1	20.2	1980	126.5	86.4	446	6.0	152	475	559	78.5	Na–Mg–Cl
80	N2	Helvetian	7.3	22.3	698	59.3	32.1	74.4	0.2	219	133	98.2	46.5	Na–Ca–SO_4
93	N3	Helvetian	7.2	24.9	857	61.4	31.3	126	1.5	207	201	127	62.4	Na–Ca–SO_4
107	N4	Helvetian	7.6	24.0	838	60.9	28.7	132	1.5	299	109	141	36.3	Na–Ca–HCO_3
112	N5	Helvetian	8.1	23.4	1031	107.5	41.8	138	7.0	176	350	136	24.3	Na–Ca–SO_4
114	N6	Helvetian	8.2	16.7	501	56.8	23.4	63.1	ND	158	50.1	76.5	39.6	Ca–Na–HCO_3
115	N7	Helvetian	8.1	21.5	427	50.1	20.5	51.4	ND	135	43	55.3	38.4	Ca–Na–HCO_3
117	N8	Helvetian	8.0	13.6	1267	170.1	44.4	156	2.3	164	377	168	115	Ca–Na–SO_4
118	N9	Helvetian	7.6	21.2	474	45.8	24.3	63.1	ND	155	28.8	72.5	44.1	Na–Ca–HCO_3
121	N10	Helvetian	8.2	23.0	2104	125.9	107.8	446	6.0	179	665	484	37.5	Na–Ca–SO_4
128	N11	Helvetian	7.3	24.2	404	30	15.8	57.1	ND	122	28.1	65.1	55.3	Na–Ca–HCO_3
253	N12	Helvetian	8.1	24.7	361	50.6	23.6	5.1	1.7	125	22.2	67.4	40.6	Ca–Mg–HCO_3
258	N13	Helvetian	7.9	25.1	618	59.5	32.6	62	1.8	165	56.9	114	90.8	Ca–Na–Cl
274	N14	Helvetian	8.0	23.5	959	67.9	39.8	84.4	1.8	257	32.9	168	60.8	Na–Ca–Cl
303	N15	Helvetian	8.1	23.5	475	47.7	31	38.5	1.7	170	40.8	86.9	34.9	Mg–Ca–HCO_3
335	N16	Helvetian	8.0	21.8	435	47.4	25.2	40.8	1.8	149	31.3	70.9	31.5	Ca–Mg–HCO_3
354	N17	Helvetian	7.8	24.0	4654	396.5	222.8	913	2.2	172	1159	1662	84.6	Na–Ca–Cl
Z1	P1	Eocene	7.5	21.6	303	58.1	8.5	12.2	1.7	152	18.8	21	31.2	Ca–Mg–HCO_3
Z2	P2	Eocene	7.7	18.6	264	50.6	5.9	8.26	1.6	147	15.6	13.7	22.3	Ca–Mg–HCO_3
J28	P3	Eocene	7.6	22.7	292	38	10	30	2.0	149	23	18	–	Ca–Na–HCO_3
J29	P4	Eocene	7.4	22.3	321	38	12	32	3.0	162	27	20	–	Ca–Na–HCO_3
J30	P5	Eocene	7.4	21.9	615	70	16	83.1	23	168	103	106	–	Na–Ca–Cl
J31	P6	Eocene	7.4	22.7	311	33	12	32	3.0	163	26	19	–	Ca–Na–HCO_3
J32	P7	Eocene	7.3	29.5	737	64	28	114	8.0	219	164	131	–	Na–Ca–Cl
J38	P8	Eocene	7.1	26.1	3065	136.1	53	869	18	251	509	1226	–	Na–Ca–Cl
HC6	P9	Eocene	7.4	22.6	559	73.9	35	25.4	1.1	280	92	42.5	7.6	Ca–Mg–HCO_3
HC7	P10	Eocene	8.4	22.5	821	64.5	71	80.5	10.3	219	147	212	15	Mg–Na–Cl
HC9	P11	Eocene	7.6	24.8	821	70.6	57.8	79.7	9.3	244	253	99.2	6.2	Mg–Ca–SO_4
HC11	P12	Eocene	8.1	24.4	862	37.3	47.7	139	14.6	329	144	145	2.7	Na–Mg–HCO_3

ND not detected, – no available data

natural to slightly alkaline conditions, while the TDS varied considerably from 265 to 4654 mg/l in the samples P2 and N17, respectively, with a mean TDS value of 925.5 mg/l. The TDS of the majority of groundwater samples are below the Syrian standard guideline value for drinking water (TDS < 1000 mg/l), and they exceed the international standard of the WHO (2011) for drinking water (TDS < 600 mg/l). Furthermore, moderate to high electrical conductivity variations from 0.35 to 6.49 mS/cm were observed in the upper and middle aquifer. The EC value increases gradually from the north to the south-western parts of Al Qweek valley and Al Matah depression. This can be explained by longer residence time of groundwater (Al-Charideh 2012) and concurrent mixing with the high salinity shallow groundwater. The intrusion of higher salinity water (Al Qweek irrigation and sewage canals) could be a reason for the elevated EC value in the south as a result of excessive pumping (Luijendijk 2003). High EC levels can be explained by dominant evaporation conditions, mineralization processes, and mixing with subsurface water horizons close to the Al Seha Marsh in the south (Abo and Merkel 2015). On the other hand, the lower EC values in the north (Jebel Simon) and eastern parts of the study area (Al Hass Mountain) may indicate an active infiltration, recharge flux downwards into shallow aquifers, and short residence time that can decrease the EC value in these regions by rainwater with lower EC than deep groundwater (Peng et al. 2014). The results also indicate that the electrical conductivities of the Helvetian and Eocene groundwater follow the general groundwater flow direction in both aquifers as shown in Fig. 4. With respect to the major ionic abundance in groundwater samples, the concentrations of the Na^{+}, Ca^{2+}, and Mg^{2+} varied considerably in the ranges of 6.28–80.7,

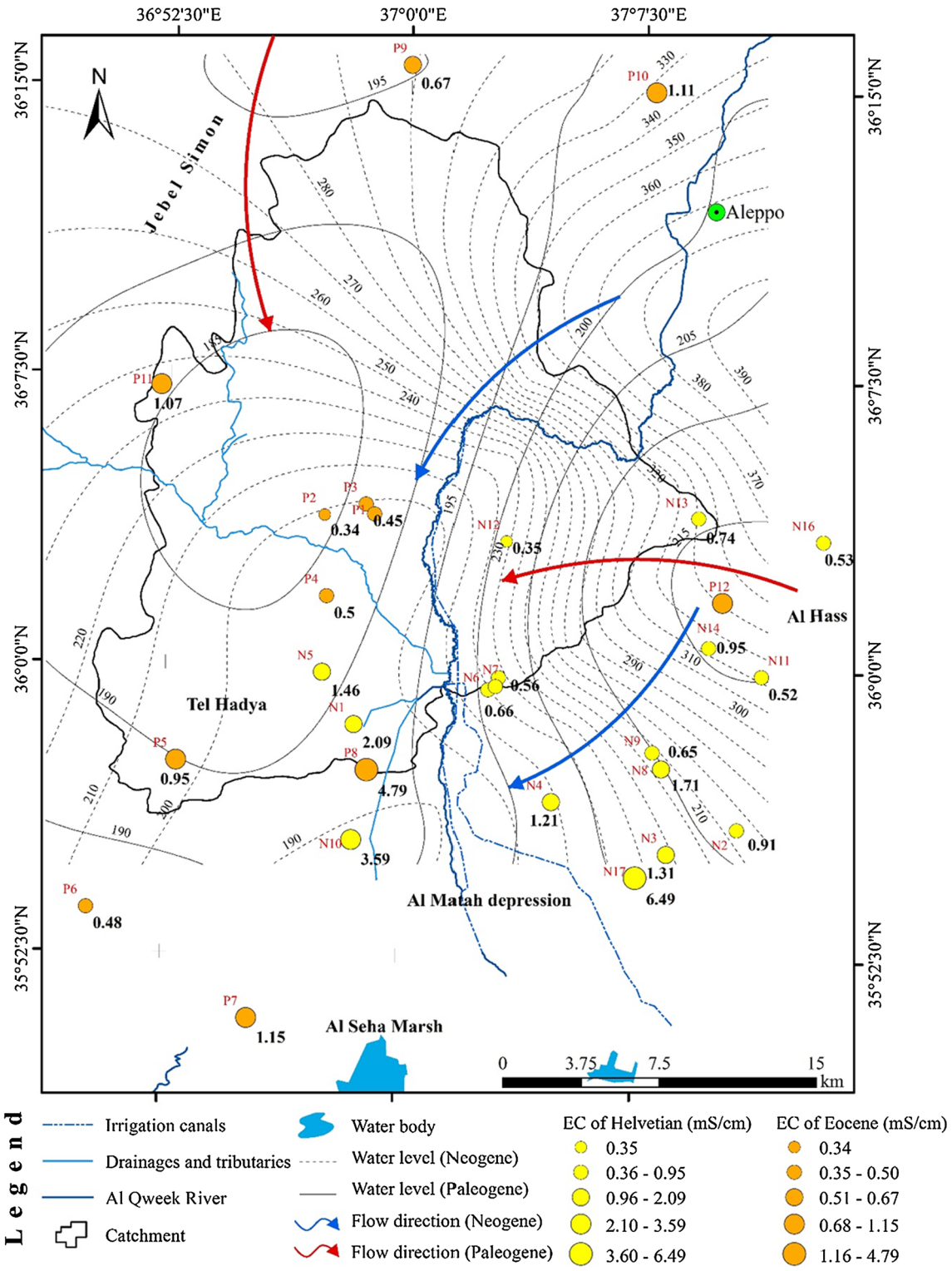

Fig. 4 Electrical conductivity of groundwater samples in the Helvetian and Eocene aquifers. The *contour lines* represent the general groundwater level of the Neogene (*dashed lines*) and the Paleogene aquifer (*continuous lines*) in the study area

12.7–76.17, and 4.9–31.4 mg/l, respectively, following the order $Na^+ > Ca^{2+} > Mg^{2+} > K^+$. On the other hand, the relative abundance of the major anions in all groundwater samples was as follows: $HCO_3^- > Cl^- > SO_4^{2-}$.

Hydrochemical facies

The results revealed that Na–Ca–HCO_3, Ca–Na–HCO_3, and Na–Ca–SO_4 are the dominant groundwater types of

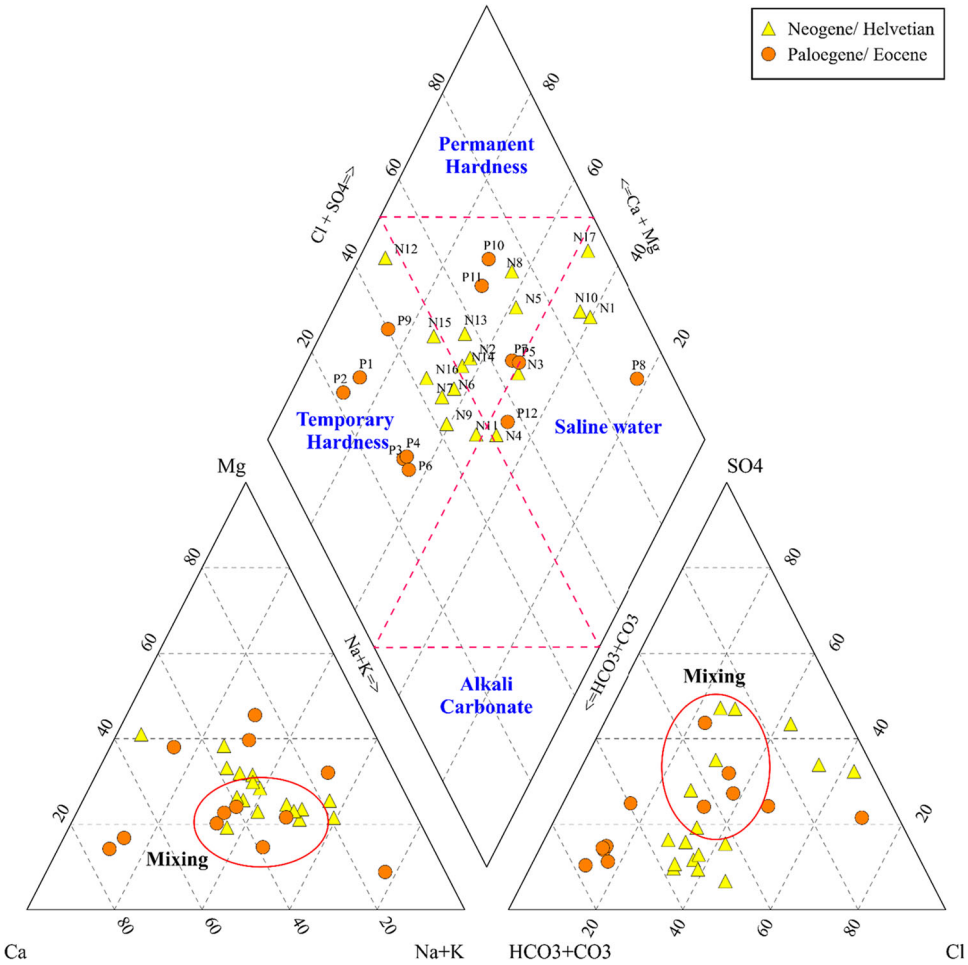

Fig. 5 Piper diagram of groundwater samples from the Neogene and Paleogene aquifers, the graphical interpretation is according to Hounslow (1995)

the Helvetian aquifer system that are distributed in the southeastern parts of the study area, and along the eastern edges of Al Qweek valley (Bredeh, Hamidi, and the Blass Villages). The results also show that the Ca–Na–Cl, Ca–Mg–HCO_3 and Ca–Na–HCO_3 water types are the main distinguished hydrochemical facies for the Eocene aquifer (Table 4). The interpretation of the Piper diagram suggests temporary hardness for groundwater samples resulting in groundwater enrichment with $Ca^{2+} + Mg^{2+}$ ions, indicating active dissolution processes of carbonate minerals in the upper and middle Eocene (samples P1, P2, and P9). The majority of groundwater samples are located in the middle part of the diamond with Ca–Mg–Cl water type. The groundwater samples on the right side of diamond suggest transition changes in the chemical constituents and an increase in the groundwater salinity to the western parts of Al Qweek valley and ICARDA site by accumulation of Na^+ and $Cl^- + SO_4{}^{2-}$ anions in the groundwater (e.g., N1, N10, P2, and P8), (Fig. 5). The Piper diagram also shows a conspicuous overlapping between the Neogene and Paleogene waters, indicating type of mixing between the both aquifers particularly in the southern parts of Al Qweek Valley (location of P5, P7, P12, N3, and N4). This occurs parallel to the groundwater flow direction from the eastern sites (samples N3, N4, and N17), to the northwest of Al Seha Marsh (location of P7) (Fig. 4). Al Bredeh fractured zone with SE–NW strikes direction may facilitate such type of groundwater mixing in the region. Furthermore, groundwater samples in the cation Piper diagram start relatively parallel to the constant magnesium line and then curves down toward to the $Na^+ + K^+$ apex. According to Hounslow (1995) and Appelo and Postma (2005), the extrapolated curve suggests that more Ca^{2+} is being exchanged than Na^+ and Mg^{2+}, and this process is accompanied with increasing of groundwater salinity.

On the other hand, the bivariate correlation test between the variables shows a significant correlation matrix between the EC, Mg^{2+}, Ca^{2+}, Na^+, Cl^-, and $SO_4{}^{2-}$ with a correlation coefficient ranging from 0.92 to 0.97 at the 0.01 P-level. Therefore, these parameters were used in groundwater clustering analysis. To eliminate abnormal trends, sample N17 was excluded from the analysis and considered as outlier. The results are shown in the dendrogram of

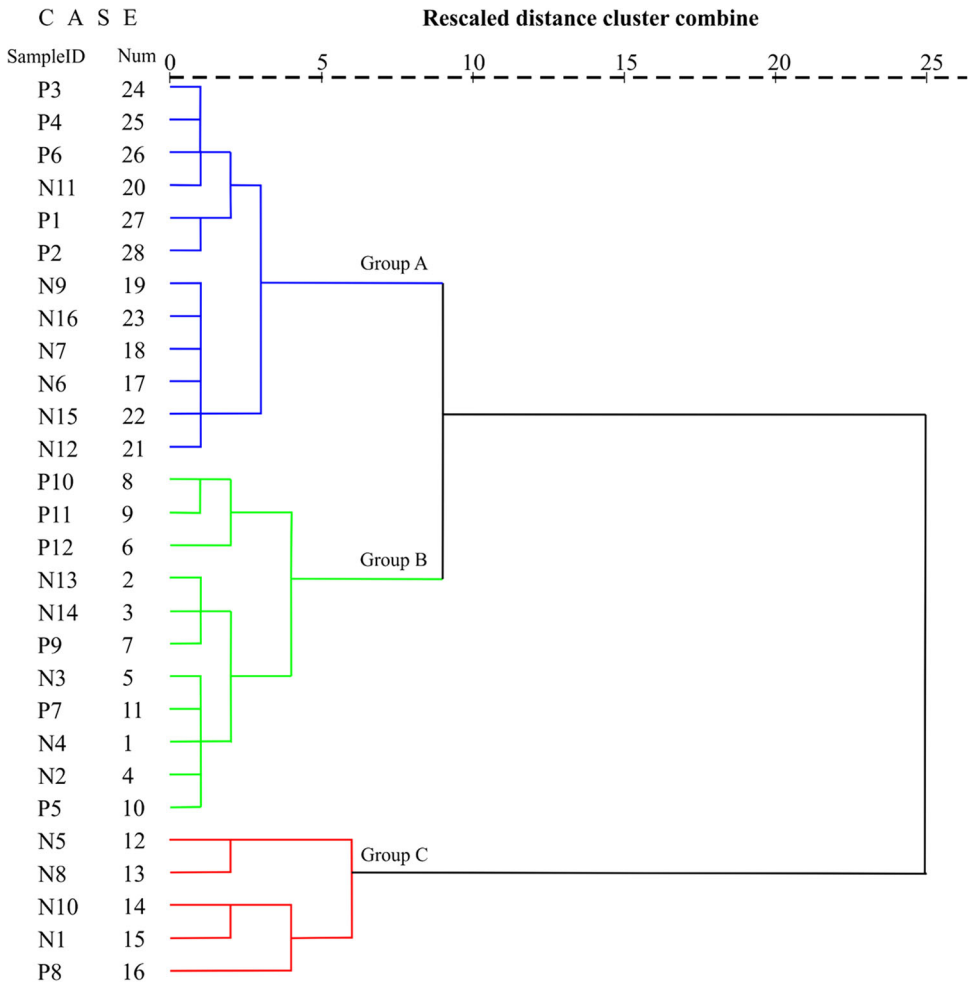

Fig. 6 Dendrogram of Q-mode cluster analysis illustrating the linkage between samples and distinguished groups from Neogene and Paleogene aquifers

Fig. 6, which revealed three primary hydrochemical facies that are selected at the Euclidean distance of 7. The groups A and B are almost identical with the scattered samples in the piper diagram. Each group show obvious similarity in the physical and chemical properties of the samples belong to Neogene and Paleogene aquifers, suggesting a hydraulic connection between these two aquifers through the developed fractures system or by excessive pumping in the area. In contrast, the third cluster (group C) forms a distinct facies characterized by high average TDS value of 1795 mg/l. The elevated TDS value can be explained by groundwater mixing of the Paleogene with higher mineralized water from deeper horizons (the upper cretaceous aquifer) as argued by Al-Charideh (2012) and Stadler et al. (2012). This type of water is mainly distributed along the southern edges of the Al Bredeh faulted zone. However, confirming that type of mixing requires adequate information about the groundwater composition and geology of the deeper aquifers. The recharge area (Al Hass) and adjoining regions (Al Zerba and Al Hader) are dominated by the groundwater group A. This type of water (group A) is considered as fresh water and characterized by relatively low average TDS of 393 mg/l. The second group B constitutes an intermediate case between the two previous hydrochemical facies (group A and C) with moderate TDS value of 742 mg/l. It is generally distributed in the northern part of the catchment close to Aleppo city, southern parts of Tel Hadya, and to southeast of Al Qweek River (Tel Dadin, Fig. 3). The result of cluster analysis and the relationship between groundwater samples in each cluster were confirmed by investigating the correlation significance. The results show significant correlation matrix with average correlation coefficients ranging from 0.98 to 0.99 in all clusters at the 0.01 P-level.

Source rock deduction

The modeled saturation indices (SI) indicate that the majority of groundwater samples are close to saturation or slightly oversaturated with respect to aragonite, calcite, and dolomite in the Helvetian aquifer, while they are generally in equilibrium with respect to the same minerals in the Eocene aquifer system, as depicted in the Fig. 7. Despite a relatively high concentration of Na^+, Cl^-, and SO_4^{2-} in

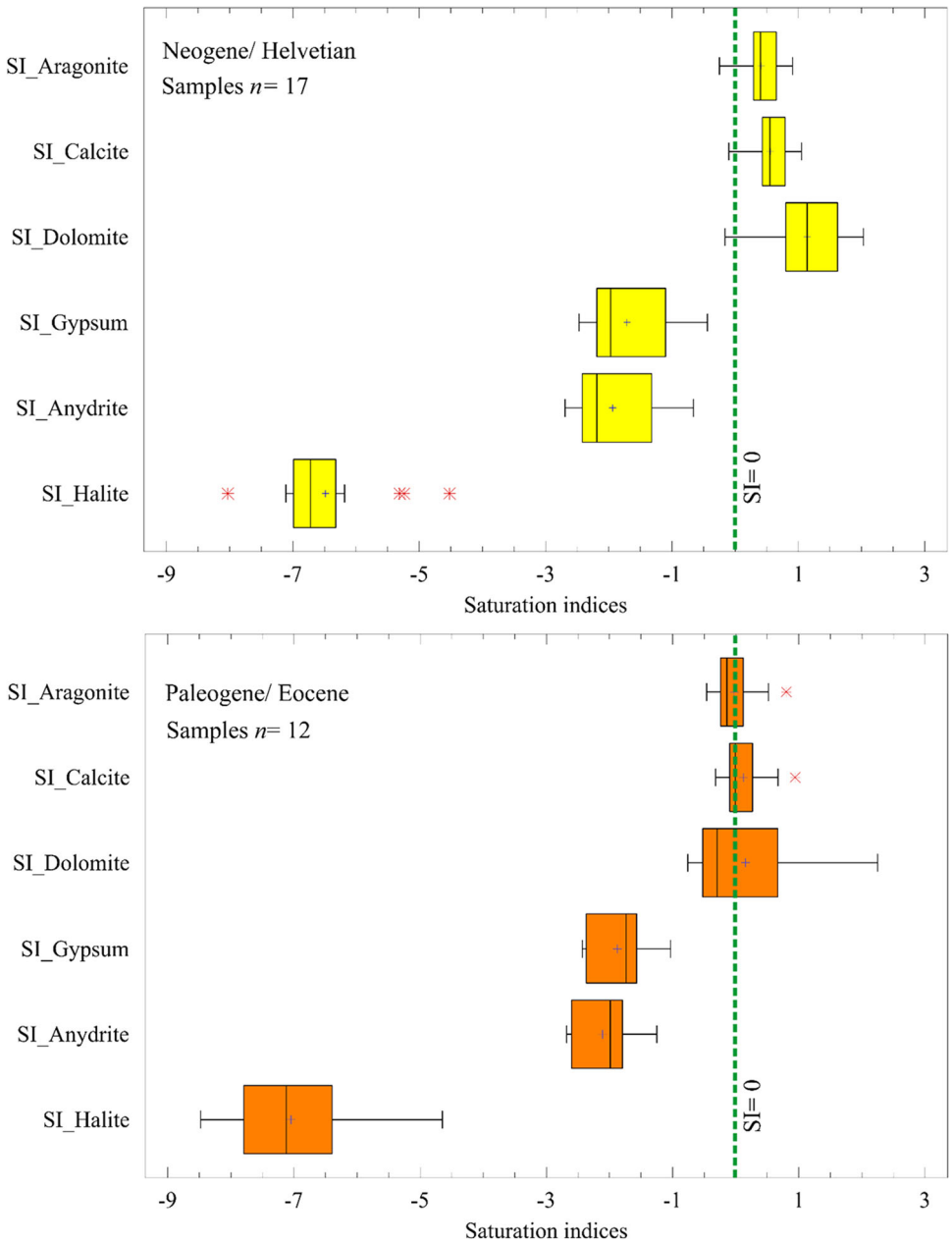

Fig. 7 Saturation indices of groundwater samples from the Neogene (Helvetian) and Paleogene (Eocene) aquifers with respect to the minerals: anhydrite, aragonite, calcite, dolomite, gypsum, and halite. The *markers in the Whisker boxes* show the lower, median, and upper quantiles. The *cross dots in the boxes* represent the mean values. *n* is the sample number per aquifer unit

most of the groundwater samples, the groundwater in both aquifers is under-saturated with respect to the halite, gypsum, and anhydrite. Table 5 lists the calculated saturation indices of groundwater samples for the Helvetian and Eocene aquifers.

Concentration of Na^+ and Cl^- ions varies from 5.1 to 913 mg/l and from 13.7 to 1663 mg/l in upper and middle aquifers, respectively. As shown in Fig. 8a, the molar Na/Cl ratio of groundwater samples is close to 1, except for the samples N1, N10, and P8. This suggests a stepwise increase of Na^+ ions in those samples, indicating possible cation exchange (natural softening) resulting along the interface surface of the clayey limestone of the Paleogene with brackish waters of the upper cretaceous. This occurs by natural ion exchange through clay minerals (Hounslow 1995). On the other hand, the excessive concentrations of Na^+ with low to moderate TDS value in the eastern parts of the catchment (N11, N14, and N16), may indicate another sources for Na^+ ions such as basalt weathering (plagioclase/albite). Similarly, most of the groundwater samples plot close to the 1:1 line with respect to Ca^{2+} and SO_4^{2-} ions. The increase of SO_4/Ca ratio scatters the samples below the equilibrium line as shown in the Fig. 8b (samples N1, N5, N10, N17, and P8). This scenario can be explained by the dissolution of gypsum and anhydrite minerals in groundwater, and calcium precipitation, and

Table 5 Saturation indices of groundwater water samples

Sample ID	Aragonite	Calcite	Dolomite	Gypsum	Anhydrite	Halite
N1	0.73	0.87	1.88	−1.02	−1.26	−5.24
N2	−0.15	−0.01	0.028	−1.63	−1.86	−6.72
N3	−0.25	−0.10	−0.16	−1.48	−1.70	−6.39
N4	0.25	0.39	0.80	−1.73	−1.95	−6.32
N5	0.91	1.05	2.03	−1.10	−1.32	−6.33
N6	0.59	0.74	1.33	−2.01	−2.25	−6.87
N7	0.53	0.67	1.27	−2.11	−2.34	−7.11
N8	0.4	0.55	0.72	−0.88	−1.14	−6.18
N9	0.65	0.79	1.62	−2.33	−2.56	−6.91
N10	0.11	0.26	0.77	−0.93	−1.16	−5.31
N11	0.29	0.44	0.94	−2.47	−2.69	−6.99
N12	0.29	0.43	0.89	−2.37	−2.59	−8.03
N13	0.38	0.52	1.14	−1.97	−2.19	−6.74
N14	0.67	0.82	1.74	−2.19	−2.42	−6.44
N15	0.50	0.65	1.45	−2.17	−2.40	−7.05
N16	0.32	0.47	0.98	−2.27	−2.50	−7.11
N17	0.78	0.92	1.94	−0.44	−0.66	−4.52
P1	−0.15	−0.01	−0.54	−2.33	−2.56	−8.14
P2	0.00	0.14	−0.37	−2.43	−2.68	−8.48
P3	−0.25	−0.11	−0.47	−2.40	−2.63	−7.82
P4	−0.39	−0.25	−0.69	−2.34	−2.57	−7.74
P5	−0.23	−0.08	−0.51	−1.63	−1.86	−6.63
P6	−0.46	−0.32	−0.76	−2.41	−2.64	−7.77
P7	−0.13	0.00	0.03	−1.53	−1.73	−6.43
P8	−0.22	−0.08	−0.22	−1.03	−1.25	−4.65
P9	0.06	0.21	0.43	−1.61	−1.91	−7.54
P10	0.8	0.94	2.25	−1.63	−1.86	−6.36
P11	0.18	0.32	0.90	−1.36	−1.58	−6.70
P12	0.52	0.67	1.79	−1.84	−2.06	−6.29

thus, excessive amounts of SO_4^{2-} remain in the groundwater. The Ca/Mg is also a very important ratio in carbonate aquifers. It is commonly used to indicate saline water intrusion, contribution of calcite and magnesium to the groundwater and cation ion exchange (Hem 1985; Rajmohan and Elango 2004). In this study, the majority of groundwater samples are distributed along and above the equilibrium line of the calcium to magnesium scatter plot, except the N1, N10, P10, P11, and P12 samples which show excessive amounts of Mg^{2+} as shown in Fig. 9. Considering the high TDS value for those samples (800–>1000 mg/l), this type of distribution (below the 1:1 line) may suggest active dissolution process of the halite layers of the Paleogene, particularly in the south and southeastern parts of the study area (Al Hoeaier and Al Blass regions, Fig. 3). The first part of the plotted samples with the Ca^{2+}/Mg^{2+} ratio approaching one for the Neogene samples, reinforces the result that calcite is being removed from the groundwater of the Paleogene and Neogene aquifers by dedolomitization or cation exchange processes of Ca^{2+} with Na^+ ions as mentioned above. According to Parkhurst and Appelo (1999), the dissolution of gypsum and anhydrite in groundwater increases the Ca^{2+} concentration and promote calcite precipitation. Consequently, CO_3^{2-} concentrations decreases, and this incites the dissolution of dolomite. On the other hand, the over-exploitation of groundwater can also enrich the water of carbonate aquifers with sulfate from deeper aquifers containing significant layers of gypsum (Cretaceous aquifer). Table 6 lists the results about source rock deduction for the groundwater of the Neogene and Paleogene aquifers using rock deduction indices suggested by Hounslow (1995). It shows that the dissolution of halite is the major source of sodium in both aquifers; the excessive amount of Na^+ in some samples indicates active cation exchange process as a result of gypsum dissolution. The results also revealed a potential plagioclase weathering in most groundwater samples in the eastern part of study area considering Na^+ to Cl^- and Ca^{2+} ratio.

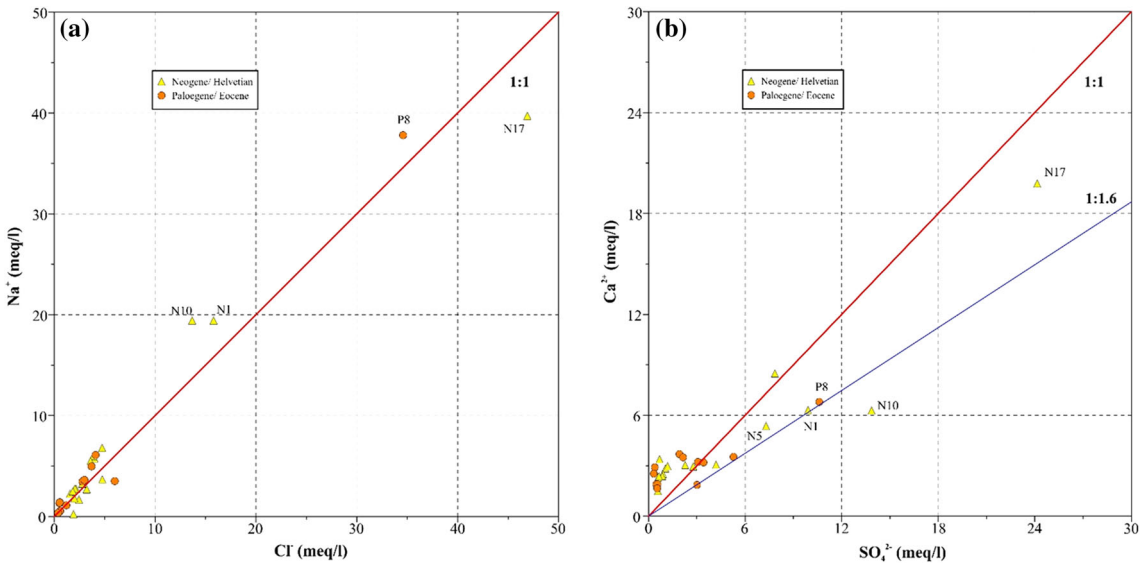

Fig. 8 Na/Cl and Ca/SO_4 relationship plot for the upper and middle aquifers

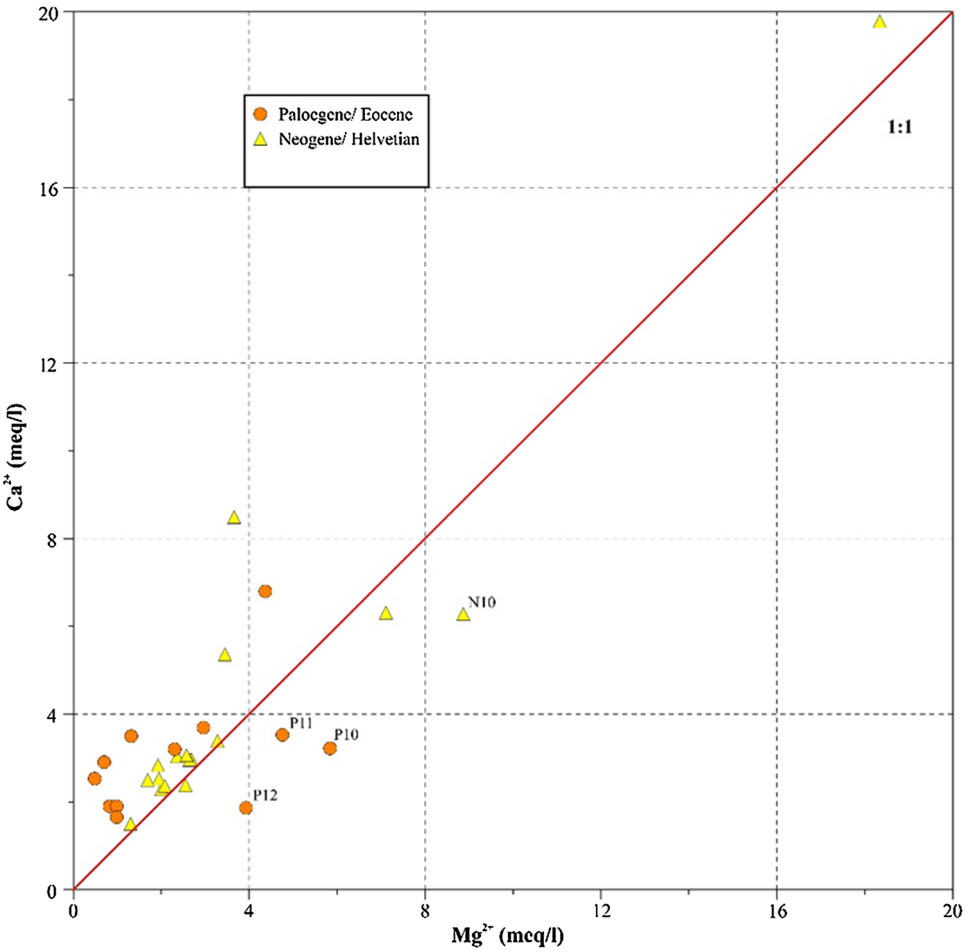

Fig. 9 Ca/Mg relationship for groundwater samples

Table 6 Source rock deductions of the neogene and paleogene water samples according to Hounslow (1995)

Aquifers	(Na + K − Cl)/(Na + K + Cl + Ca)			Na/(Na + Cl), TDS considered			Ca/(Ca + SO_4), pH considered			TDS (mg/l)			Cl^-/∑anions, TDS considered			HCO_3^-/∑anions		
	Min	Max	Mean	Min	Max	Mean	Min	Max	Mean	Min	Max	Mean	Min	Max	Mean	Min	Max	Mean
Neogene/Helvetian																		
Values	−1.96	0.49	−0.73	0.10	0.61	0.35	0.32	0.84	0.58	361	4654	2507	0.29	0.73	0.51	0.04	0.44	0.24
Predicted source rocks	Plagioclase weathering possible			Sodium source other than halite- albite, ion exchange possible			Calcium source other than gypsum -carbonate or silicates			Carbonate weathering or brine or seawater			Rock weathering expected			Intrusion of brackish water or brine		
Samples	N2, N3, N4, N5, N7, N8, N9, N10 and N11			All except N12, N13, N14			Except N2, N3, N8, N10			All except N7, N9, N11, N12, N15, N16			–			All except N17		
Source rocks of other samples	–			Revers softening, brackish water intrusion			Gypsum dissolution and calcium removal/ion exchange or calcite precipitation			Silicate weathering expected			–			Gypsum dissolution		
Paleogene/Eocene																		
Values	−2.97	0.53	−1.21	0.36	0.72	0.54	0.38	0.88	0.63	265	3065	1665	0.11	0.78	0.45	0.09	0.76	0.43
Predicted source rocks	Plagioclase weathering possible			Sodium source other than halite-albite, ion exchange			Calcium source other than gypsum, carbonate, or silicates			Carbonate weathering or brine or seawater			Rock weathering expected			Intrusion of brackish water or brine		
Samples	P3, P4, P6, P9, P12			All except P9, P10			Except P7, P8, P10, P11			All except P1, P2, P3, P4, P6			–			–		
Source rocks of other samples	–			Revers softening, brackish water intrusion			Gypsum dissolution and calcium removal/ion exchange or calcite precipitation			Silicate weathering expected			–			–		

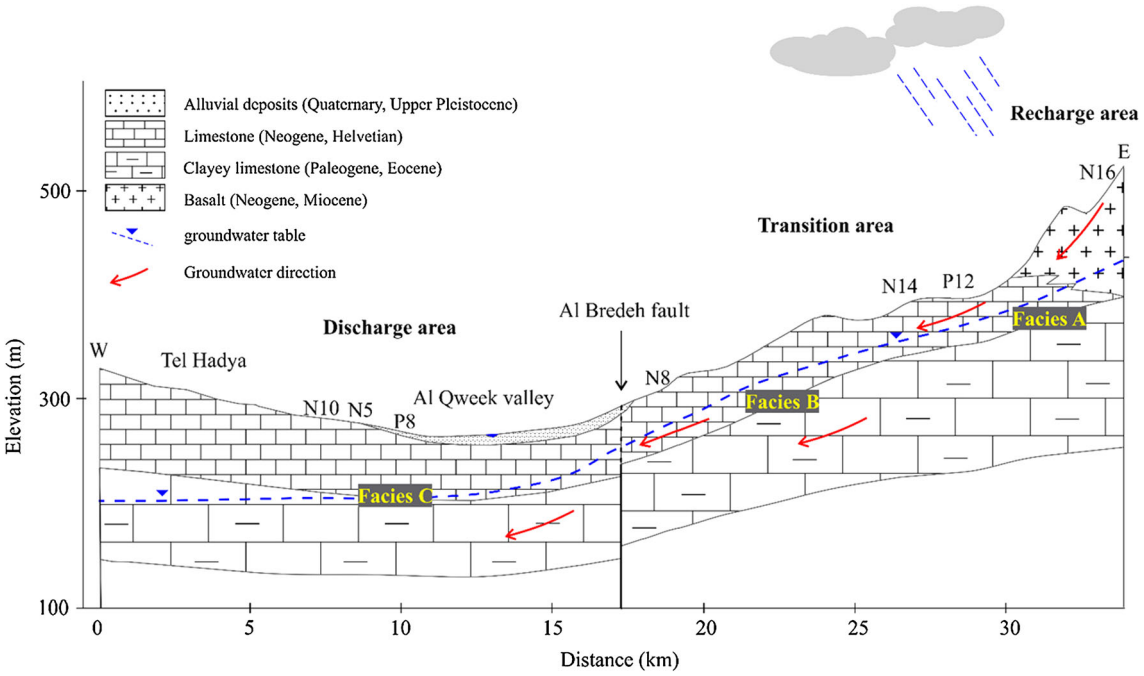

Fig. 10 Conceptual hydrogeological and hydrogeochemical cross-section based on the geology, hydrogeology, and geochemical results

Table 7 The calculated phase mole transfers in the inverse geochemical modeling using phreeqc.dat

Phase mole transfers (mol/l)					
Recharge area (precipitation + group A)		From group A to B		From group B to C	
Phases 1		Phases 2		Phases 3	
Ca-montmorillonite	-2.05×10^{-03}	Dolomite	4.07×10^{-04}	Dolomite	3.80×10^{-04}
Plagioclase	3.46×10^{-03}	Calcite	-3.94×10^{-04}	Calcite	-1.22×10^{-03}
Hypersthene	2.44×10^{-04}	Gypsum	2.66×10^{-04}	Gypsum	5.08×10^{-03}
Hematite	-1.60×10^{-04}	Halite	1.21×10^{-03}	Halite	7.44×10^{-04}
Diopside	1.02×10^{-04}	CH_2O	–	CH_2O	3.18×10^{-03}
$CO_{2(g)}$	8.80×10^{-04}	$O_{2(g)}$	1.22×10^{-03}	$CO_{2(g)}$	–
CaX_2	5.36×10^{-04}	CaX_2	1.44×10^{-04}	CaX_2	-1.48×10^{-03}
NaX	-1.07×10^{-03}	NaX	-2.87×10^{-04}	NaX	2.9×10^{-03}

Positive numbers of mineral mass transfers indicate dissolution, while negative values indicate precipitation. The positive numbers of the cation exchange indicate a decrease in calcium or magnesium and an increase in sodium concentration in groundwater

Inverse modeling and groundwater evolution

Figure 10 shows the conceptual cross-section along the flowpath and the main hydrochemical facies in the region. The results of geochemical inverse modeling summarize three main geochemical processes that dominate the groundwater evolution in the study area. The plagioclase weathering of the Miocene basalt in the recharge area, the preliminary de-dolomitization, and ion exchange processes along the transition zone between recharge area and water type B, and concurrent reverse cation exchange/de-dolomitization along the flowpath between the hydrochemical facies B and C. Table 7 lists the calculated phase mole transfers of different minerals and cation exchange along the groundwater flowpaths.

The results indicate that basalt weathering in the eastern part of the study area is a potential source for excessive sodium in the water group A resulting by a dissolution of albite and hypersthene minerals and cation exchange (Ca^{2+} is being removed and Na^{+} released). The phase mole transfers were estimated by 2.4×10^{-04} and 3.4×10^{-03} for the plagioclase and hypersthene minerals, respectively. In contrast, hematite, and Ca-montmorillonite are being removed from water by precipitation in

form of clay minerals. This model suggests the following reaction:

$$\begin{aligned}&\text{Recharge water} + \text{Silicate minerals}\\&\quad(\text{Plagioclase, Hypersthene, and Diopside}) + \text{Hematite}\\&\quad + CO_{2(g)} + O_{2(g)} \rightarrow \text{water type A}\\&\quad + \text{Ca-montmorillonite (clay minerals) formation.}\end{aligned}$$

The first geochemical flowpath (A to B) suggests primary de-dolomitization process with active cation exchange in the Helvetian limestone. This is evidently reflected by dissolution of dolomite and gypsum, and precipitation of calcite (calcite phase mole transfer $= -3.94e^{-04}$) coincided with cation exchange of calcium and sodium on the hosting formation (positive CaX_2). This scenario can be described as follows:

$$\begin{aligned}&\text{Water type A} + \text{Calcite} + \text{Dolomite} + \text{Halite} + \text{Gypsum}\\&\quad + \text{Ion exchange } (CaX_2 \text{ and NaX})\\&\quad + CO_{2(g)} \rightarrow \text{water type B}\\&\quad + \text{increased } Na^{+} \text{ by cation exchange and de-dolomitization.}\end{aligned}$$

On the other hand, dissolution of dolomite, gypsum, and halite, and precipitation of calcite are the dominant processes controlling the water composition in the southwestern parts of the region (hydrochemical facies C). This is consistent with gradually increase of TDS value along the flowpaths from the eastern to the western part of the study area. Conversely to the second scenario (flowpath A to B), the results indicate reverse cation exchange in groundwater by progressive release of calcium and decrease in sodium ions (negative exchange value CaX_2). This could be explained by an interface between sodium-rich water (group C) and clayey limestone in the first and second aquifer, where sodium concentration is suggested to be higher than clay-exchange equilibrium concentration (Hounslow 1995). Accordingly, the end-member groundwater evolution can be described by the following reaction:

$$\begin{aligned}&\text{Water type B} + \text{Calcite} + \text{Dolomite} + \text{Gypsum} + \text{Halite}\\&\quad + \text{Ion exchange } (CaX_2 \text{ and NaX}) + CH_2O\\&\quad + CO_{2(g)} \rightarrow \text{water type C}\\&\quad + \text{increased } Na^{+} \text{ by cation exchange and de-dolomitization.}\end{aligned}$$

Groundwater suitability for drinking and irrigation

According to the USEPA (2002) and WHO (2011) guidelines for drinking water, groundwater of the upper aquifer is not recommended for human consumption due to the levels of the total dissolved solids (TDS > 600 mg/l), except for some of the groundwater found in the eastern and parts of the study area (Al Hader and Al Blass region). However, the majority of groundwater samples are below the Syrian threshold for drinking water of 1000 mg/l.

The hydrochemical analysis also showed elevated concentrations of nitrate in all groundwater samples ranging from 24.4 to 116 mg/l in the ICARDA region and Hamidi village, respectively (N5, N8, and N9 on the map), Fig. 11. This can be a consequence of anthropogenic contamination resulting from overuse of chemical fertilizers, return flow irrigation or mixing of groundwater with wastewater of unprotected sewage canals in the region. In contrast, the Paleogene aquifer exhibits better water quality with a relatively lower TDS value than in most groundwater samples, except the areas close to the Makhala village (P8, Fig. 3). According to the Syrian guidelines for drinking water WHO (2006), nitrate is found below the maximum contamination limit (MCL) of 44 mg/l and thus below the national threshold value. However, caution is required by groundwater exploitation form the Paleogene aquifer as well.

From the agricultural point of view, groundwater with TDS value ranges from 500 to 1500 mg/l and an electrical conductivity (EC) ranges from 0.77 to 2.25 mS/cm is considered as moderate salinity water, with adverse effects to moderately sensitive crops such as wheat, barley, legumes, grasses, and forage (Maas and Hoffman 1977; Ayers and Westcot 1985; Shalhevet 1994). In the present study, groundwater samples show medium salinity hazard with respect to the TDS and EC values. As shown in the Wilcox diagram (Fig. 12), the analyzed water samples are found in the range of medium to high salinity and low sodium hazard (C2–C3 and S1), except for the N1, N10, and P8 samples which exhibit high–very high salinity and medium sodium hazard (C3–C4, S2) or very high salinity/sodium hazard values (C4–S4). The minimum and maximum values of calculated SAR in the study area range from 0.14 to 9.1 and 0.29 to 16 for the Neogene and Paleogene groundwater samples, respectively. Generally, groundwater with medium and low salinity (C2–S1) can be used in irrigation for most crops, while water samples with high salinity and low sodium hazard (C3–S1) can be applied in irrigation with caution in medium-textured soils (Latif and El Kashouty 2010). Therefore, groundwater in the Banos and Hoeaier area (southeast of ICARDA region, Figure 3) is not recommended for irrigation activities due to its potentially harmful effects on the soil structure and crop yields in the long term. Groundwater in this region requires chemical treatment and good drainage to enhance its quality and to remove excessive salts.

Essential groundwater criteria for irrigation purposes in the study area are listed in Table 8. Furthermore, the results show that the average exchangeable sodium ratios (ESR) in all groundwater samples are above their limit and reach up to 0.7, except the samples (P1, P2 and P9) in the north and central part of the region. This indicates relatively high

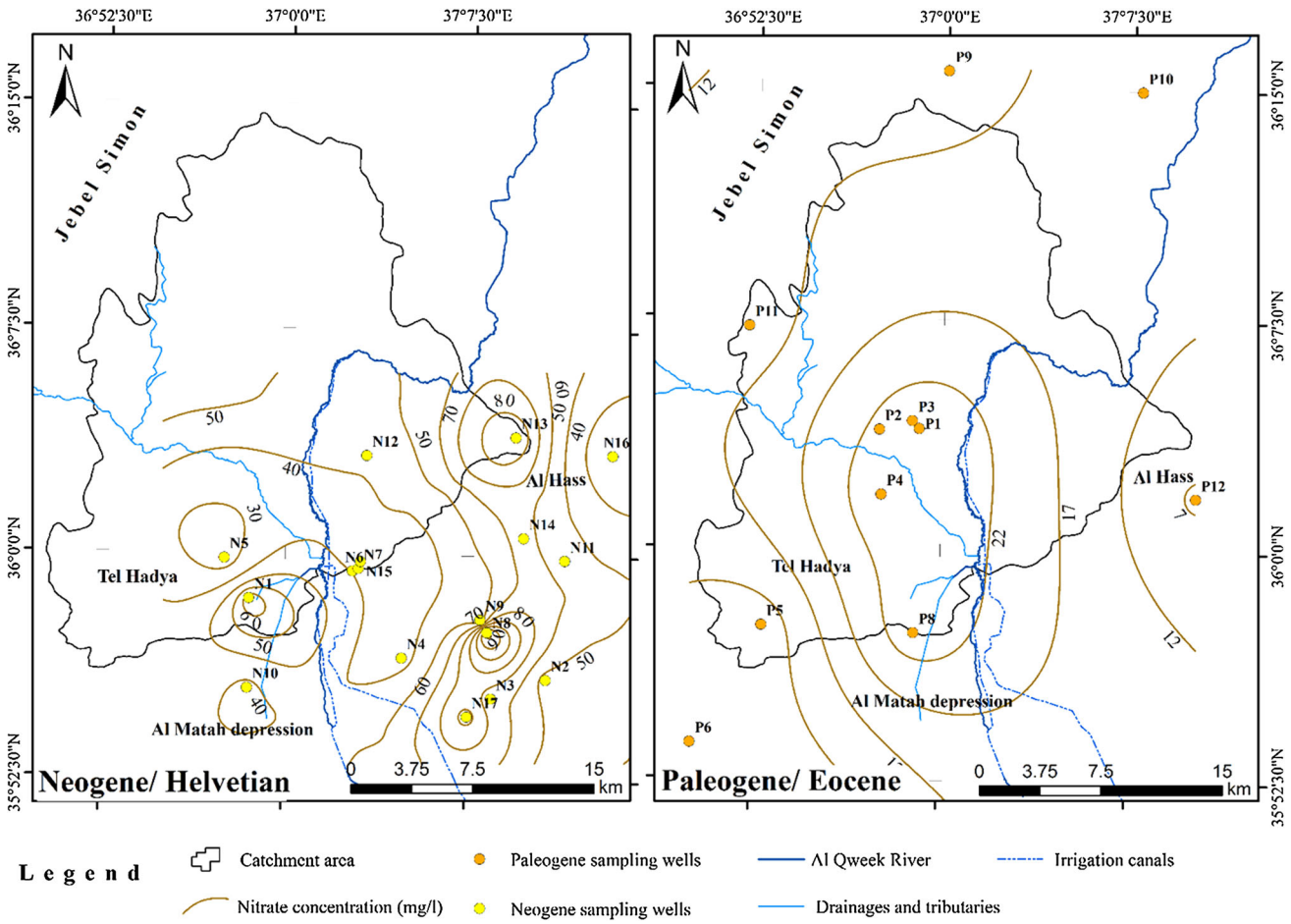

Fig. 11 Nitrate distribution in the Helvetian and Eocene aquifers

tendency of Na^+ and $Ca^{2+}+ Mg^{2+}$ ions to exchange in the soil leading to negative effects on both soil texture and crop productivity. On the other hand, the MH in groundwater samples varied from 30.1 to 58.5 and 16.1 to 67.9 % for the Neogene and Paleogene aquifer systems. However, the majority of groundwater samples were found below or close to the 50 % MH, except for the N10, P10, P11, and P12 samples which are out of scale and could be considered as not recommended sources for irrigation water. The elevated MH value in these areas could be explained by a dissolution process of the dolomite or a basic ion exchange. As shown in Table 8, most of the groundwater samples have negative, low RSC with an average value of −3.72, suggesting an improbable buildup of sodium in the soils due to a sufficient amount of Mg^{2+} and Ca^{2+} in the water.

Conclusion and recommendations

The study emphasizes the need to use several techniques to comprehend the hydrogeological system and the potential geochemical processes in groundwater such as the geochemical inverse modeling and statistical approaches coupled to the traditional graphical methods. Three groundwater groups were distinguished in the study area based on their concerted chemical properties. Group A exhibits fresh groundwater criteria with low TDS of 393 mg/l and Ca–Mg–HCO_3 water type, Group B with relatively moderate TDS (∼750 mg/l) and dominant Na^+ and Mg^{2+} ionic concentration, and water group C with an elevated average TDS of 1700 mg/l. The plagioclase weathering, de-dolomitization, and cation exchange processes are the dominant geochemical processes control the groundwater evolution along the flow paths. These processes lead to continuous increase in groundwater salinity to the southwestern part of the study area. From the irrigation point of view, the groundwater in the region is not recommended for the sensitive and moderate sensitive crops. Due to the lack of hydrochemical data such as trace elements in groundwater and soil's chemical composition further investigations are required. Investigating mixing proportion between the Neogene and Paleogene aquifers is recommended for further investigation. One option could to use stable

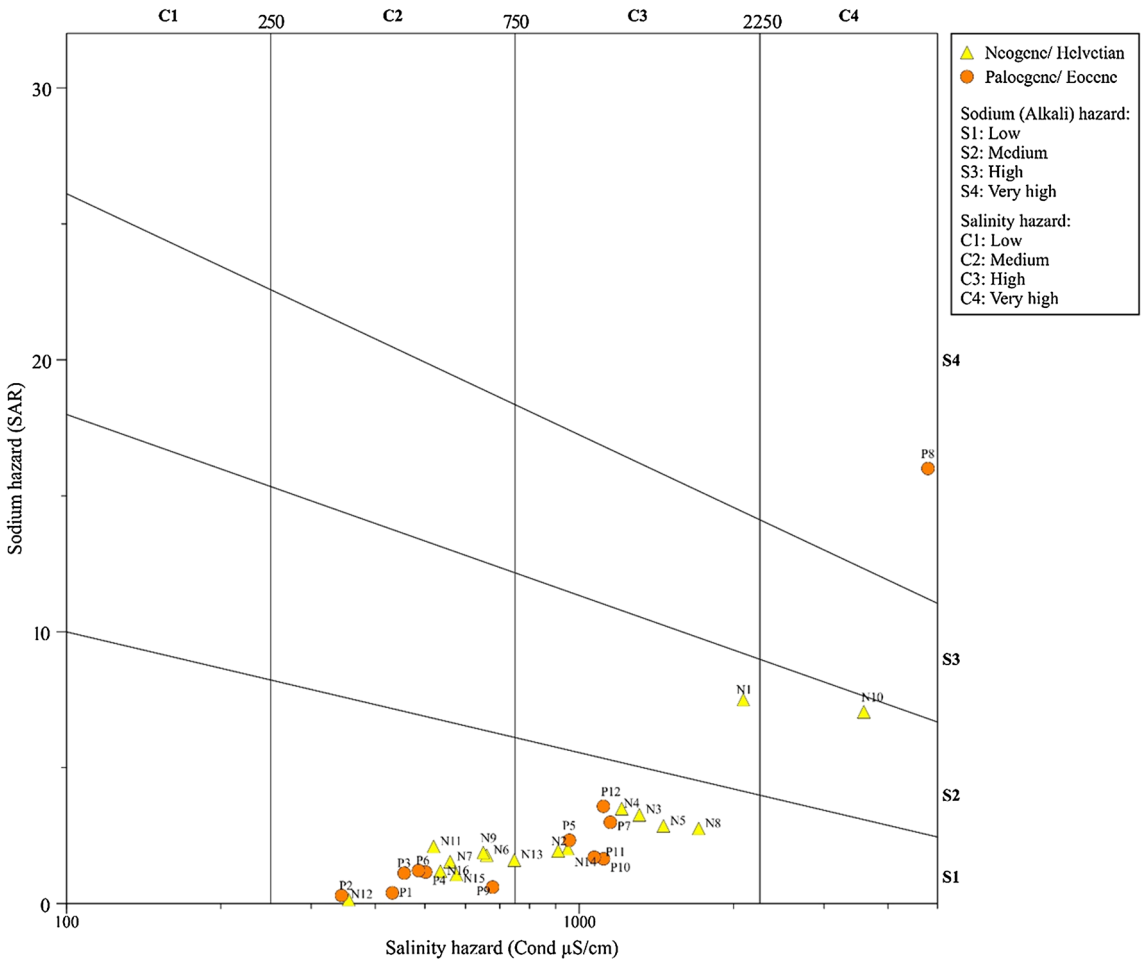

Fig. 12 Wilcox diagram depicts the sodium adsorption ratio (SAR) and the salinity hazard (SH) of groundwater sample from the Paleogene and Neogene aquifer systems

Table 8 The assessment of groundwater suitability for irrigation purposes based on potential hazard indices

Sample ID	SAR	ESR	MH %	RSC	SH	Sample ID	SAR	ESR	MH %	RSC	SH
N1	7.50	1.44	53.0	−9.92	High	N16	1.19	0.39	46.8	−1.00	Medium
N2	1.94	0.57	47.2	−1.20	High	N17	9.10	1.04	48.1	−34.60	Very high
N3	3.26	0.97	45.7	−1.45	High	P1	0.39	0.14	30.3	−1.11	Medium
N4	3.49	1.06	43.7	0.20	High	P2	0.29	0.11	34.2	−0.60	Medium
N5	2.86	0.68	39.1	−4.51	High	P3	1.12	0.48	30.3	−0.28	Medium
N6	1.78	0.57	40.5	−1.36	Medium	P4	1.16	0.48	34.2	−0.23	Medium
N7	1.54	0.53	40.3	−1.17	Medium	P5	2.33	0.75	27.4	−2.06	High
N8	2.76	0.56	30.1	−8.05	High	P6	1.21	0.52	37.5	0.04	Medium
N9	1.87	0.64	46.6	−0.74	Medium	P7	2.99	0.9	41.9	−1.91	High
N10	7.06	1.28	58.5	−10.80	Very high	P8	16.0	3.38	39.1	−7.04	Very high
N11	2.10	0.88	46.4	−0.20	Medium	P9	0.60	0.16	44.5	−2.05	Medium
N12	0.14	0.05	43.5	−1.93	Medium	P10	1.65	0.38	64.5	−5.46	High
N13	1.60	0.47	47.4	−2.40	Medium	P11	1.70	0.41	57.4	−4.28	High
N14	2.01	0.55	49.1	−1.85	High	P12	3.58	1.05	67.9	−0.39	High
N15	1.07	0.34	51.7	−1.64	Medium	Avg.	2.90	0.71	43.37	−3.72	High

isotopes ^{18}O and ^{2}H liked for inverse geochemical modeling with PHREEQC.

Acknowledgments The authors thank the Syrian Ministry of Irrigation (MOI) and the Federal Institute for Geosciences and Natural Resources (BGR) for providing the data. Special thanks are also due to Prof. Dr. Adriana Bruggeman, Dr. Elco Luijendijk, and Mr. Fabian Helms for their appreciated support and providing data for this work.

References

Abo RK, Merkel BJ (2015) Comparative estimation of the potential groundwater recharge in Al Zerba catchment of Aleppo basin, Syria. Arab J Geosci 8(3):1339–1360. doi:10.1007/s12517-013-1222-9

Al-Charideh A (2012) Geochemical and isotopic characterization of groundwater from shallow and deep limestone aquifers system of Aleppo basin (north Syria). Environ Earth Sci 65(4):1157–1168

Appelo CAJ, Postma D (2005) Geochemistry, groundwater and pollution. CRC Press, Boca Raton

Asiwaju-Bello YA, Olabode FO, Duvbiama OA, Iyamu JO, Adeyemo AA, Onigbinde MT (2013) Hydrochemical evaluation of groundwater in Akure Area, south-western Nigeria, for irrigation purpose. Eur Int J Sci Technol 2(8):235–249

Ayers RS, Westcot DW (1985) Water quality for agriculture, vol 29. Food and Agriculture Organization of the United Nations FAO, Rome

Ball JW, Nordstrom DK, Zachmann DW (1987) WATEQ 4 F—a personal computer FORTRAN translation of the geochemical model WATEQ 2 with revised data base. Available from Books and Open File Report Section, USGS Box 25425, Denver, CO 80225 USGS Open-File Report 87-50, 1987 108 p, 2 tab, 26 ref, 2 append

Berndtsson R, Mourad KA (2012) Water status in the Syrian water basins. Open J Mod Hydrol 2(1):15–20

BGR, MOI (2004) Initial assessment study of water sector management in the Syrian Arab republic. Federal Ministry of Economic Cooperation and Development BGR & Syria Ministry of Irrigation BGR, Damascus

Brew G, Barazangi M, Al-Maleh AK, Sawaf T (2001) Tectonic and geologic evolution of Syria. Geo Arabia 6:573–616

Carucci V, Petitta M, Aravena R (2012) Interaction between shallow and deep aquifers in the Tivoli Plain (Central Italy) enhanced by groundwater extraction: a multi-isotope approach and geochemical modeling. Appl Geochem 27(1):266–280

Custodio E (2002) Aquifer overexploitation: what does it mean? Hydrogeol J 10(2):254–277

Droubi A (1983) Study of water resources in the Dawwa Basin, part 2, chap 6. Hydrochemistry report. The Arab Center for the Studies of Arid Zones and Dry Lands, Syria (ACSAD), Damascus

Eaton FM (1950) Significance of carbonates in irrigation waters. Soil Sci 69(2):123–134

Edmunds WM (2003) Renewable and non-renewable groundwater in semi-arid and arid regions. In: Abdulrahman SA, Warren WW (eds) Developments in water science, vol 50. Elsevier, Amsterdam, pp 265–280. doi:10.1016/S0167-5648(03)80023-0

Edmunds W, Droubi A (1998) Groundwater salinity and environmental change. In: Isotope techniques in the study of environmental change

Freeze RA, Cherry JA (1979) Groundwater. Prentice-Hall Inc, Englewood Cliffs

GCHS (1999) Hydrogeological investigations of Aleppo Basin, Phase 1. General Company of Hydraulic Studies Homs, Syria

Gibbs RJ (1970) Mechanisms controlling world water chemistry. Science 170(3962):1088–1090

Gruzgiprovodkhoz (1982) Hydrogeological and hydrological surveys and investigations in four areas of the Syrian Arab Republic. Georgian State Institute for Design of Water Resource, Tbilisi

Hagi-Bishow M (1998) Assessment of LEACHM-C Model for semi-arid saline irrigation. McGill University, Quebec

Harron W, Webster G, Cairns R (1983) Relationship between exchangeable sodium and sodium adsorption ratio in a solonetzic soil association. Can J Soil Sci 63(3):461–467

Hem JD (1985) Study and interpretation of the chemical characteristics of natural water, vol. 2254. Department of the Interior, US Geological Survey

Hiscock K, Bense V (2014) Hydrogeology: principles and practice. Wiley, Chichester

Hopkins BG, Horneck DA, Steven RG, Ellsworth JW, Sullivan DM (2007) Managing irrigation water quality for crop production in the Pacific Northwest. Oregon State University, Oregon

Hounslow A (1995) Water quality data: analysis and interpretation. CRC Press, Boca Raton

ICARDA (2000) Syria: geology and derived aquifer location and properties, scale 1:1,500,000. Annex to Research Report "An Overview of the Water Resources in Syria" prepared by R. Hoogeveen, E. De Pauw within the framework of the Natural Resource Management Program, sponsored by USAID-CGIAR Linkage Fund, GIS handling by A. Oberle, A. Balikian, B. Nseir. Aleppo

JICA (1997) The study on water resource development in the northwestern and central basin in the Syrian Arab Republic (phase 1). Sanyu Consultants Inc., Tokyo

Joshi DM, Kumar A, Agrawal N (2009) Assessment of the irrigation water quality of river Ganga in Haridwar district. Rasayan J Chem 2(2):285–292

Kalf FR, Woolley DR (2005) Applicability and methodology of determining sustainable yield in groundwater systems. Hydrogeol J 13(1):295–312

Latif AA, El Kashouty M (2010) Groundwater investigation in Awlad Salameh, Southern Sohag, Upper Egypt. GEOCIENCIAS 14:1

Li P, Wu J, Qian H (2013) Assessment of groundwater quality for irrigation purposes and identification of hydrogeochemical evolution mechanisms in Pengyang County, China. Environ Earth Sci 69(7):2211–2225

Lloyd JW, Heathcote J (1985) Natural inorganic hydrochemistry in relation to groundwater. Clarendon Press, Oxford

Luijendijk E (2003) Groundwater resources of the Aleppo basin, Syria. MSc Thesis, Vrije Universiteit Amsterdam, The Netherlands

Luijendijk E, Bruggeman A (2008) Groundwater resources in the Jabal Al Hass region, northwest Syria: an assessment of past use and future potential. Hydrogeol J 16(3):511–530

Ma GS-K, Malpas J, Suzuki K, Lo C-H, Wang K-L, Iizuka Y, Xenophontos C (2013) Evolution and origin of the Miocene intraplate basalts on the Aleppo Plateau, NW Syria. Chem Geol 335:149–171

Maas E, Hoffman G (1977) Crop salt tolerance—current assessment. J Irrig Drain Div 103(2):115–134

Nishanthiny SC, Thushyanthy M, Barathithasan T, Saravanan S (2010) Irrigation water quality based on hydro chemical analysis, Jaffna, Sri Lanka. Am-Eurasian J Agric Environ Sci 7:100–102

Paliwal KV (1972) Irrigation with saline water. Monogram no. 2, vol. 2. Water Technology Centre, Indian Agricultural Research Institute IARI, New Delhi, p. 198

Parkhurst DL, Appelo C (1999) User's guide to PHREEQC (Version 2): a computer program for speciation, batch-reaction, one-dimensional transport, and inverse geochemical calculations

Peng T-R, Lu W-C, Chen K-Y, Zhan W-J, Liu T-K (2014) Groundwater-recharge connectivity between a hills-and-plains' area of western Taiwan using water isotopes and electrical conductivity. J Hydrol 517:226–235. doi:10.1016/j.jhydrol.2014.05.010

Piper AM (1944) A graphic procedure in the geochemical interpretation of water-analyses. Trans Am Geophys Union 25:914–928

Plummer LN, Back W (1980) The mass balance approach; application to interpreting the chemical evolution of hydrologic systems. Am J Sci 280(2):130–142

Ponikarov V (1964) Geological map of Syria, scale 1:200,000. Sheets J-37-1, II; I-37-XX and I-37-XIX. Technoexport, Moscow

Prasad A, Kumar D, Singh DV (2001) Effect of residual sodium carbonate in irrigation water on the soil sodication and yield of palmarosa (*Cymbopogon martinni*) and lemongrass (*Cymbopogon flexuosus*). Agric Water Manag 50(3):161–172. doi:10.1016/S0378-3774(01)00103-2

Rajmohan N, Elango L (2004) Identification and evolution of hydrogeochemical processes in the groundwater environment in an area of the Palar and Cheyyar River Basins, Southern India. Environ Geol 46(1):47–61

Richards LA (1954) Diagnosis and improvement of saline and alkali soils. Soil Sci 78(2):154

Ryan J, Estefan G, Rashid A (2001) Soil and plant analysis laboratory manual, 2nd edn. International Center for Agricultural Research in the Dry Areas (ICARDA) and the National Agricultural Research Center (NARC), Aleppo

Sadashivaiah C, Ramakrishnaiah C, Ranganna G (2008) Hydrochemical analysis and evaluation of groundwater quality in Tumkur Taluk, Karnataka State, India. Int J Environ Res Public Health 5(3):158–164

Selkhozpromexport (1979) Hydrogeological and hydrogeological surveys and investigations in four areas of Syrian Arab Republic; Hydrogeology book 1. Text, vol 2. Georgian State Institute for Design of Water Resources Development projects, Gruzgiprovodkhoz, Tbilisi

Shalhevet J (1994) Using water of marginal quality for crop production: major issues. Agric Water Manag 25(3):233–269

Stadler S, Geyh M, Ploethner D, Koeniger P (2012) The deep Cretaceous aquifer in the Aleppo and Steppe basins of Syria: assessment of the meteoric origin and geographic source of the groundwater. Hydrogeol J 20(6):1007–1026

Szabolcs I, Darab C (1964) The influence of irrigation water of high sodium carbonate content on soils. In: Proceedings of 8th international congress of ISSS, Trans, II. pp 803–812

UN-ESCWA (1997) Report on mission to Syria Arab Republic (During the period 10–20 June 1997—hydrogeologic advice to ICARDA on sustainable agricultural groundwater management in dry areas). ESCWA, Beirut

USEPA (2002) National recommended water quality criteria. Environmental Protection Agency, Washington, DC

WHO (2006) A compendium of drinking-water quality standards in the Eastern Mediterranean Region. Regional Centre for Environmental Health Activities, Cairo

WHO (2011) Guidelines for drinking-water quality, 4th edn. World Health Organization, Malta

Wolfart R (1966) Zur Geologie und Hydrogeologie von Syrien: unter besonderer Berücksichtigung der süd-und nordwestlichen Landesteile, vol 68. Bundesanstalt f, Bodenforschung